Mesoscale Numerical Study of Two Cases of Long-Lived Quasi-Stationary Convective Systems over Eastern Spain

R. ROMERO AND C. A. DOSWELL III

National Severe Storms Laboratory, NOAA/ERL, Norman, Oklahoma

C. RAMIS

Meteorology Group, Departament de Física, Universitat de les Illes Balears, Palma de Mallorca, Spain

(Manuscript received 29 October 1999, in final form 17 March 2000)

ABSTRACT

A set of mesoscale numerical simulations using the Pennsylvania State University–National Center for Atmospheric Research model is used to investigate two cases of extreme precipitation over eastern Spain. Both cases (3–4 November 1987 and 20 October 1982) were characterized by quasi-stationary mesoscale convective systems that developed over the Valencia region and lasted more than 30 and 12 h, respectively. Rainfall totals in 24 h exceeded 800 mm on 3–4 November and 400 mm on 20 October at some localities of that region. The first event occurred within a weak and very stagnant synoptic pattern under a persistent easterly/northeasterly low-level jet stream impinging on the Valencian orography. In contrast, the second case involved a westward-moving surface low driven by an upper-level jet streak, which evolved along the northern edge of an upper-level cutoff low over North Africa. In both cases, the mesoscale model forecast spatial details of the precipitation field reasonably accurately, as well as capturing its long duration, but underestimated the storm total precipitation. Model output fields suggest that the development of a surface mesolow by latent heat release, as well as lee cyclogenesis induced by the Atlas Mountains, could have played an important role in both events by providing low-level convergence and enhanced upslope winds. Thus, a factor separation technique is used to explore this issue. For the event of 3–4 November 1987, latent heat is decisive for explaining the precipitation maximum over central Valencia, and the Atlas orography induces rainfall enhancement over the same zone. For the event of 20 October 1982, the latent heat release is again shown to be important, whereas the Atlas Mountains orography factor appears to inhibit rainfall. This is the first time that it has been documented that the Atlas-induced modulation of the surface pressure field is not a positive factor for heavy precipitations over eastern Spain. This exceptional case may be due to a negative interaction between the Atlas Mountains and the upper-level dynamics and frontal forcing for this event.

1. Introduction

Among all severe convective weather situations, fall season heavy rainfall represents the most threatening phenomenon in the western Mediterranean region, depicted in Fig. 1. Devastating flash floods occur every year somewhere in eastern Spain, southern France, Italy, or North Africa, being responsible for a great proportion of the fatalities, property losses, and destruction of infrastructure caused by natural hazards. These events tend to be most frequent and intense during the fall (Font 1983) because the Mediterranean Sea is quite warm after the high insolation of the summer, thereby ensuring considerable moisture supply and low static stability in the overlying air.

Riosalido (1990) has shown that most of the flash flood events in the region can be attributed to quasi-stationary mesoscale convective systems (MCSs). Within such systems, individual convective storm cells may move rapidly, but the area where storms attain maturity and produce heavy rain can remain nearly stationary. Included among the examples of extreme rainfalls produced by quasi-stationary systems are 450 mm recorded during 24 h in Alforja (south Catalonia) on 10 October 1994, almost 300 mm in 24 h in the Piedmont region (northwestern Italy) on 5 November 1995, 220 mm in 3 h in the vicinity of Vaison-La-Romaine city (southern France) on 22 September 1992, and the well-known Biescas event in northeastern Spain (7 August 1996), in which 225 mm in 3 h fell in the mountains of this locality, resulting in 86 fatalities.

As noted by Chappell (1986), the rapid genesis of

Corresponding author address: Dr. Romualdo Romero, National Severe Storms Laboratory, NOAA/ERL, 1313 Halley Circle, Norman, OK 73069.
E-mail: rromero@enterprise.nssl.noaa.gov

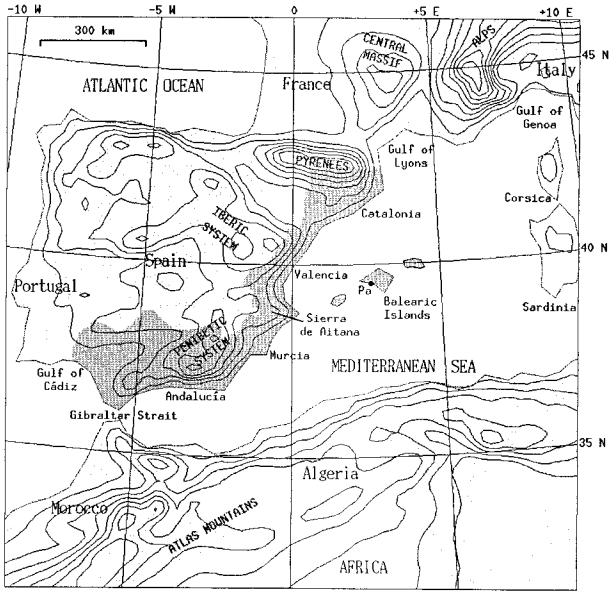

FIG. 1. Depiction of the western Mediterranean region, with an indication of geographical locations and mountain systems mentioned in the text. Smoothed orography is contoured at 250-m intervals, starting at 250 m.

convective cells in a specific region as older cells dissipate downstream (propagation effect), which is necessary for an MCS to become stationary, requires an initiating mechanism to release the potential buoyant energy repeatedly in the same location relative to the storm. Synoptic-scale ingredients such as upward vertical motion, water vapor flux convergence at low levels, high water vapor content in a deep atmospheric column, and potential or latent instability (Maddox et al. 1979) are required to ensure continuous replenishment of buoyant energy, whereas mesoscale processes focus those ingredients in specific zones and provide the necessary lifting mechanisms for low-level parcels (Doswell 1987). Mesoscale lifting mechanisms include convective outflow boundaries, mesoscale zones of boundary layer convergence (Weaver 1979) (fronts, drylines, orographically induced vortices, blocking, etc.), ageostrophic motion associated with short-wave troughs or jet streaks at upper levels (Rockwood and Maddox 1988), interaction between upper jet streaks (Hakim and Uccellini 1992), gravity waves (Uccellini 1975), motions driven by conditional symmetric instability (Emanuel 1983), coupling of upper and lower jet streaks (Uccellini and Johnson 1979), and orographic lifting in areas of complex terrain (Maddox et al. 1978). As long as synoptic and mesoscale ingredients remain favorable during several hours over a specific region, convection can be continuously generated in a relatively small area and the convective system can become long lived and quasi-stationary.

In the western Mediterranean region, topographic forcing exerts a dominant influence on the meteorological systems at a wide range of spatial scales. In particular, the complex and high coastal mountains that surround the western Mediterranean sea (notably the Alps, Pyrenees, and Atlas Mountains; Fig. 1) have been shown to be decisive for the intensity and spatial localization of heavy rainfalls (e.g., Romero 1998). Over eastern Spain, mechanical ascent provided by upslope flow over local terrain features, as well as the actions of the Pyrenees (for Catalonia and northern Valencia) and Atlas Mountains (especially for Valencia, Balearic Islands, Murcia and eastern Andalucía), which promote upward motion, have long been recognized as playing essential roles in producing heavy rainfalls. Diagnostic studies (e.g., Ramis et al. 1994) supported by numerical experiments (Ramis et al. 1998) have illustrated the importance of the mesohigh induced over northeastern Spain by the blocking action of the Pyrenees under southeasterly flows. The influence of this mesohigh can be enhanced by a low pressure center to the south, which augments the onshore wind component, helping to focus convection over the coastal areas of northeastern Spain. Numerical simulations, combined with subjective surface mesoscale analyses (Romero et al. 1997; Ramis et al. 1998), also have illustrated the potentially important role of the surface mesolow and warm air tongue induced by the Atlas Mountains when the downstream section of the synoptic-scale midtropospheric trough occurs across those mountains. These mesoscale structures, which extend leeward over the Algerian coast and western Mediterranean, imply additional sources of low-level convergence, as well as enhanced easterly flow and warm advection toward eastern Spain. Since synoptic environments leading to heavy precipitation in eastern Spain often are not strongly forced (as indicated by the absence of strong and well-defined large-scale forcing for upward motion in the mid- and upper troposphere), mesoscale features such as those described above can dominate the development and evolution of convection (Stensrud and Fritsch 1993).

In this paper, we consider two exceptional cases of long-lived quasi-stationary convective systems over eastern Spain. The first MCS (3–4 November 1987) persisted for 33 h, remaining nearly stationary during all that time over the Valencia region. The second MCS (20 October 1982), larger in size but shorter in lifetime (about 12 h), affected the southeastern regions of Spain in general, but with its maximum rainfall occurring over interior Valencia. Rainfall in 24 h exceeded 800 and 400 mm, respectively, in the proximities of the Sierra de Aitana (see Fig. 1), producing two of the most catastrophic flash floods in the recent history of Valencia. Mesoscale numerical simulations are used to identify potential mesoscale mechanisms that could explain the extraordinary stationarity and efficiency of both MCSs. Also, the simulations are useful to explore the value of mesoscale numerical models for operational forecasting of this type of events in the western Mediterranean. It should be noted that, to date, high-resolution models

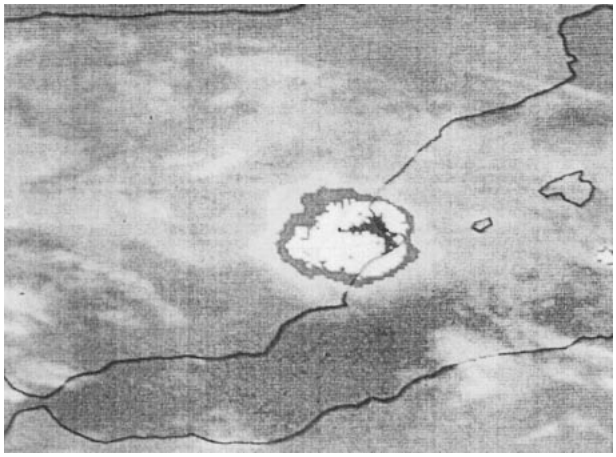

FIG. 2. Infrared Meteosat picture at 0530 UTC 4 Nov 1987. Dark gray, white, and black represent temperatures lower than −42°, −54°, and −64°C, respectively.

have not been extensively used in the western Mediterranean countries on an operational basis.

Following this introduction, in section 2 we present an overview of the events and a description of the synoptic environment in which they occurred. The model physical parameterizations and characteristics of the simulations are outlined in section 3. Section 4 focuses on the identification of mesoscale ingredients relevant to both events, which is completed in section 5 with a factor separation study. Conclusions and discussion are contained in section 6.

2. Overview of the events and synoptic environment

a. Gandía case

About 0300 UTC 3 November 1987, convection began over the waters of the Gulf of Valencia, very close to the coastline. During the subsequent hours, the convective system grew in size and extended farther inland, remaining virtually anchored in central Valencia (Fig. 2) until 1200 UTC 4 November, dissipating rapidly thereafter. During its 33-h life cycle, the MCS remained mostly isolated from other smaller and mobile convective systems that developed over southeastern Spain and western Mediterranean sea, until 0230 UTC 4 November. At that time, another MCS approaching from the southwest that had originated 4 h before (through the merger of two convective systems that began over Murcia and Penibetic system) merged with the central Valencia MCS (Fernández et al. 1995). After the merger, the MCS attained its maximum size (~200 km diameter) and a nearly circular shape (Fig. 2).

The high stationarity and long life of the main MCS are clearly reflected in the presence, on both 3 and 4 November, of a wide area in Valencia with 24-h rainfall[1] exceeding 60 mm (Fig. 3). Embedded within this general area, there are two rainfall maxima of about 250 mm, one over Sierra de Aitana and the other north of these mountains. Farther south, other important centers of precipitation appear on both days, caused by convection that developed over Murcia and eastern Andalucía. Cumulative amounts computed from the previous rainfall analyses, including the main MCS formative stage (isohyets not shown), slightly exceed 600 mm at some points of Valencia. This value is an underestimate of the actual peak rainfall, owing to the density of the rain gauges available for the analyses (see Fig. 4). The observed rainfall maximum for this event was recorded in Gandía (Valencia) and exceeded 1000 mm in 36 h, with 400 mm in only 6 h (Riosalido et al. 1988), 36-h amounts that had never been recorded in Spain. Hereinafter, we will refer to this case as the Gandía case.

An inspection of National Centers for Environmental Prediction (NCEP) analyses reveals that a midtropospheric cold-core closed low, already present on 1 November, moved progressively from the Atlantic toward the northeast until it was situated about the Gulf of Cádiz at the early hours of 3 November. Then, it remained stationary for more than 24 h until 1200 UTC 4 November, after which time it continued eastward and dissipated rapidly. Meanwhile, a slow-moving blocking anticyclone centered over the British Isles intensified appreciably. Such a configuration, with an anticyclone poleward of the cyclone (Fig. 5a), sometimes referred to as ''Rex block'' pattern, was present at all tropospheric levels, defining a nearly equivalent barotropic vertical structure. At 250 hPa, two upper-level jet streaks (ULJSs) were present at Mediterranean latitudes, one over southern Italy and Greece and the other over Morocco (Fig. 5a). However, these features appear not to have influenced the environment in the Valencia area very strongly. Indeed, calculation of quasigeostrophic dynamical forcing (not shown) demonstrates that significant upward forcing at middle and upper levels was only present over North Africa and southern Spain, and only marginally affected Valencia. Therefore, vertical destabilization in the area where the MCS developed cannot be described as a rapid response to the synoptic-scale forcing, unlike, for example, cases of approaching short-wave troughs for which quasigeostrophic forcing is typically strong, concentrated, and vertically coherent. In this case, the synoptic-scale processes acted rather slowly, but at the same time guaranteed conditions for deep convection in eastern Spain during many hours or even days, as opposed to the more transient effects associated with strong, mobile synoptic patterns. The

[1] The standard climatological rain gauge network in Spain measures 24-h rainfall from 0700 UTC to 0700 UTC the next day.

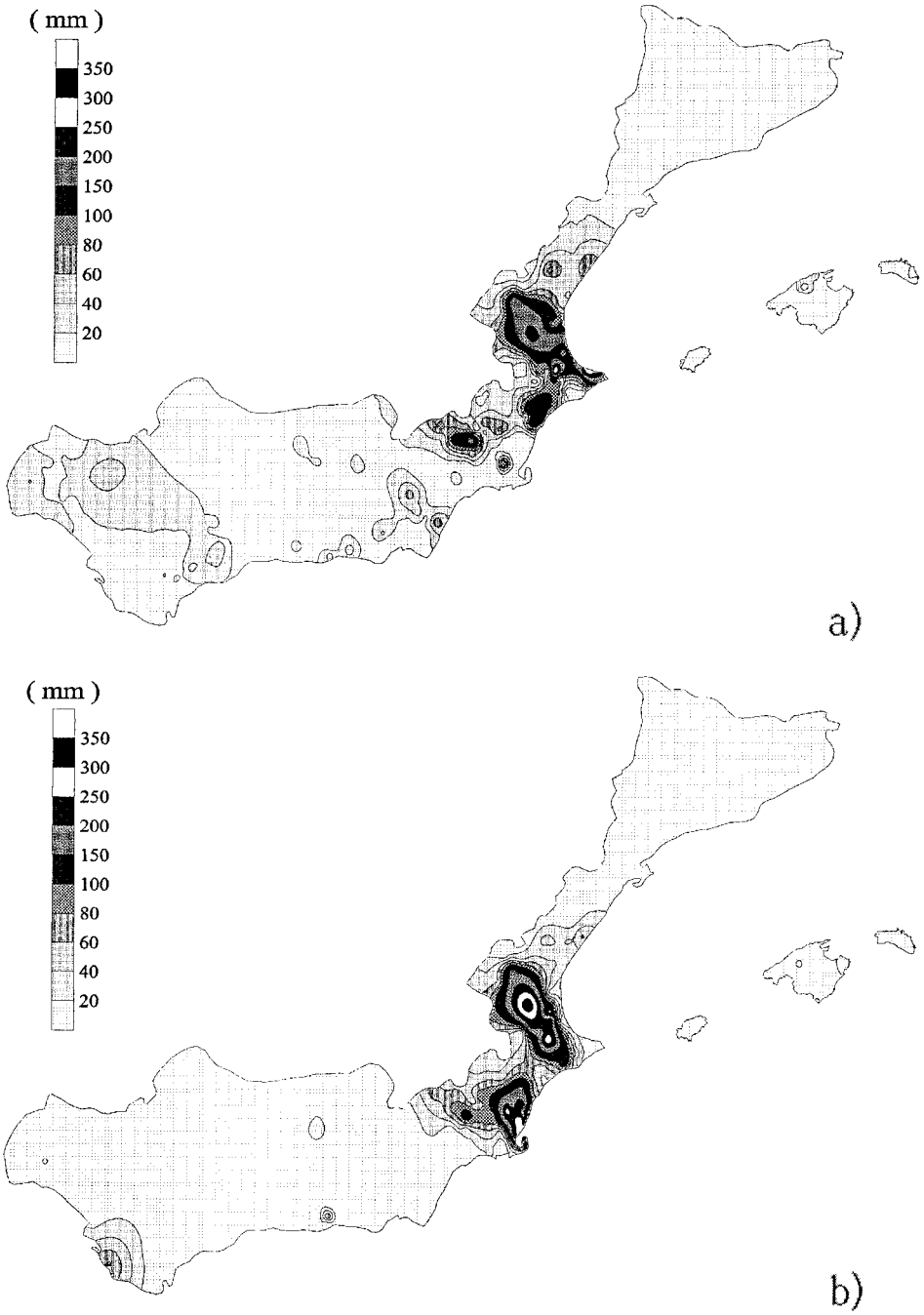

FIG. 3. Analysis of the observed rainfall (mm) in Mediterranean Spain (dark shaded region in Fig. 1) (a) from 0700 UTC 3 Nov to 0700 UTC 4 Nov 1987 and (b) from 0700 UTC 4 Nov to 0700 UTC 5 Nov 1987.

lack of strong and well-defined large-scale forcing at upper levels is a common feature of the flash flood events in eastern Spain (e.g., Doswell et al. 1998), though not a general rule. For example, Homar et al. (1999) have shown that the coupling of two upper-tropospheric jet streaks was essential for the development and movement of a MCS over the Valencia area.

At low levels, the low pressure area centered over the Gulf of Cádiz was elongated along the Algerian coast, with a secondary low pressure center south of the Balearic Islands (Fig. 5b). This mesoscale feature is a common leeside effect when the mid- and upper-tropospheric flow overrides the Atlas Mountains from the south. As indicated by theory (e.g., Smith 1989), the inter-

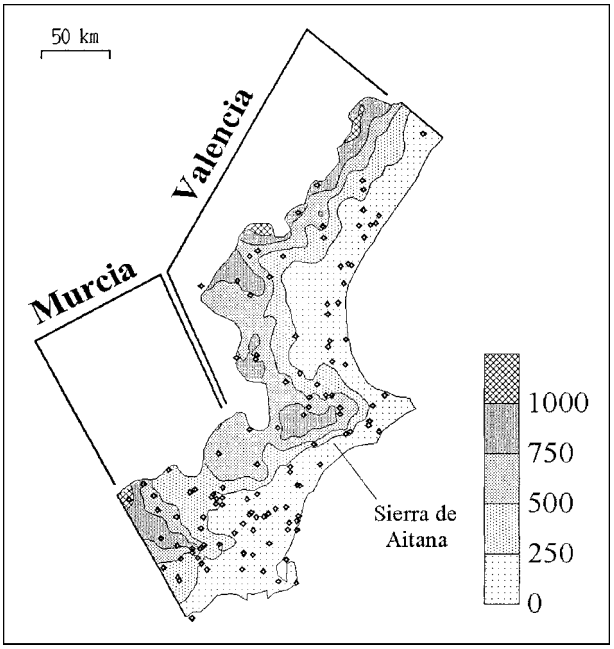

FIG. 4. Spatial distribution of rain gauges in Valencia and Murcia (Fig. 1) used for the rainfall analysis. The local orography (m) is also included.

action between airflow and a mountain ridge is strongest when the upper-level winds are intense and nearly perpendicular to the ridge axis, as occurs for the Atlas Mountains when troughs are located to the west (Fig. 5a). Since the development of low pressure centers off the Algerian coast implies an increase of the north–south pressure gradient somewhere over the western Mediterranean, this results in an enhancement of the easterly geostrophic advection of warm and moist air toward certain zones of eastern Spain. Thus, within the broad scenario characterized by an upstream trough or closed low aloft and general easterly flow at low levels interacting with the coastal orography of eastern Spain, the action of the Atlas Mountains usually has been considered an important ingredient for the focusing and maintenance of convection (Romero et al. 1997; Ramis et al. 1998).

As seen in Fig. 5b, a northeasterly low-level jet stream (LLJS) extending from Corsica to Valencia was present at low levels. It should be noted that orographic rainfall enhancement by the Sierra de Aitana is maximized for that wind direction (Romero et al. 1999). As the British Isles anticyclone intensified, the LLJS and the associated downstream convergence over the Valencia region became progressively stronger. Also, the low-level temperature field reveals a stationary baroclinic zone over the Mediterranean, separating warm, moist air of African origin from colder and drier air injected by the anticyclone from continental Europe. This baroclinic zone is visible on satellite pictures as a general cloudy mass stretched along the E–W direction (Fig. 2). The

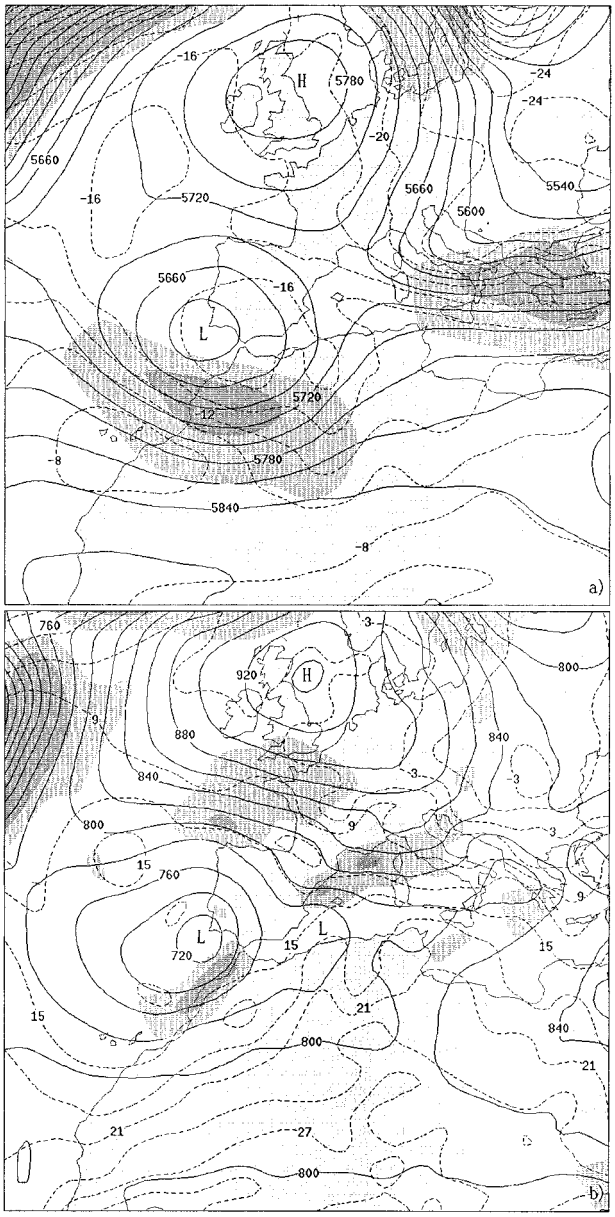

FIG. 5. Synoptic situation at 1200 UTC 3 Nov 1987. (a) Geopotential height (gpm, continuous line) and temperature (°C, dashed line) at 500 hPa, and horizontal wind speed at 250 hPa greater than 30 m s^{-1} (light shaded) and 40 m s^{-1} (dark shaded). (b) Geopotential height (gpm, continuous line), temperature (°C, dashed line), and horizontal wind speed greater than 10 and 15 m s^{-1} (light and dark shaded, respectively), at 925 hPa. Lows and highs mentioned in the text are indicated.

deep convection of Valencia developed along the western end of this zone, under the influence of the intensifying LLJS established between the deep anticyclone to the north and the Atlas-induced low to the south. These features persisted during many hours, owing to the stationary nature of the synoptic-scale flow pattern.

A sounding of the mediterranean air mass in which the deep convection of Valencia developed can be ob-

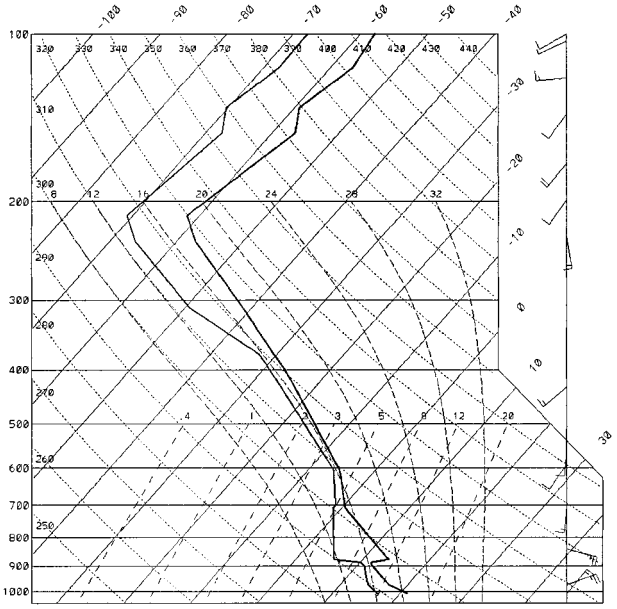

FIG. 6. Radiosounding on 1200 UTC 3 Nov 1987 at Palma (Pa in Fig. 1).

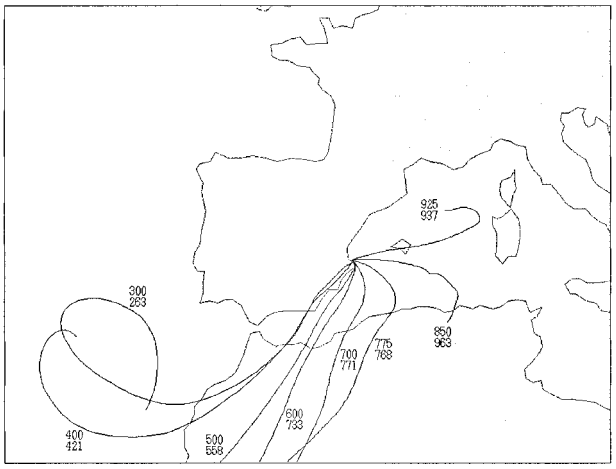

FIG. 7. Two-day back trajectories starting at 0000 UTC 4 Nov 1987 of parcels located over the coast of central Valencia. Upper and lower labels indicate the pressure of the parcels over Valencia and at the source regions, respectively.

tained from Palma, a station located in the Balearic Islands (Pa in Fig. 1). At 1200 UTC 3 November (Fig. 6), the sounding yields a convective available potential energy (CAPE) for the surface parcel of 909 J kg^{-1}, a convective inhibition (CIN) of 12 J kg^{-1}, a lifted index (LI) of 0, a *K* index (K) of 31, a total total's index (TT) of 47, and high humidity in all the troposphere resulting in 35 mm of precipitable water (PW). The winds reflect the speed maximum about 900 hPa as well as significant directional shear in the lower troposphere motivated by the Atlas-induced low. Aloft, however, these winds are very weak. A significant feature of the sounding is the presence of a lid structure (Farrell and Carlson 1989), with the thermal inversion located right above 900 hPa. Such a structure is a common characteristic of the flash flood events in eastern Spain, being caused by the ascent of relatively well-mixed air coming from the elevated African continent above the surface maritime air (Ramis et al. 1998). To illustrate this point, we have calculated back trajectories for parcels located above the Valencia coast, using initialized gridded analyses of the wind field from the European Centre for Medium-Range Weather Forecasts. The trajectory plot (Fig. 7) confirms that the source airstream of the low-level parcels is from the east, with a long path over the Mediterranean, whereas the parcels at higher levels arrive from the south after a long path over the dry, heated African lands.

b. Tous case

The MCS of 20 October 1982 developed in the early hours of the day and remained in the same geographical location almost 12 h. As seen in Fig. 8, this MCS was greater in areal extent than the Gandía system, since its cloud shield nearly covered all the southeastern quadrant of the Iberian Peninsula. Rivera and Riosalido (1986) determined that this system met the mesoscale convective complex (MCC) criteria proposed by Maddox (1980), the first time that the genesis and evolution of a MCC was documented in Europe.

The MCC produced significant precipitation in most areas of southeastern Spain, but again the major rainfall and most intense floods occurred in the Valencia region (Fig. 9). An extensive area with more than 100 mm and peak values about 250 mm was observed north of the Sierra de Aitana on the rainfall analysis of 19 and 20 October (Figs. 9a and 9b, respectively, each one encompassing approximately half of the MCC lifetime). Important amounts of precipitation also occurred south of the Sierra de Aitana on 19 October, and in northern Valencia on 20 October, as the convective activity

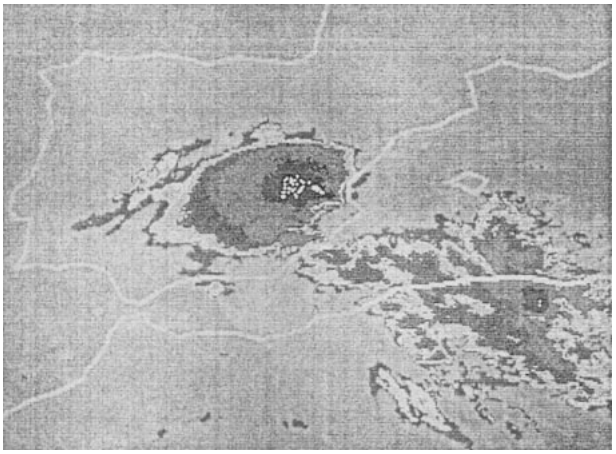

FIG. 8. Infrared Meteosat picture at 0800 UTC 20 Oct 1982. Enhanced grays are used for temperatures lower than −30°C, with white corresponding to −60°C approximately.

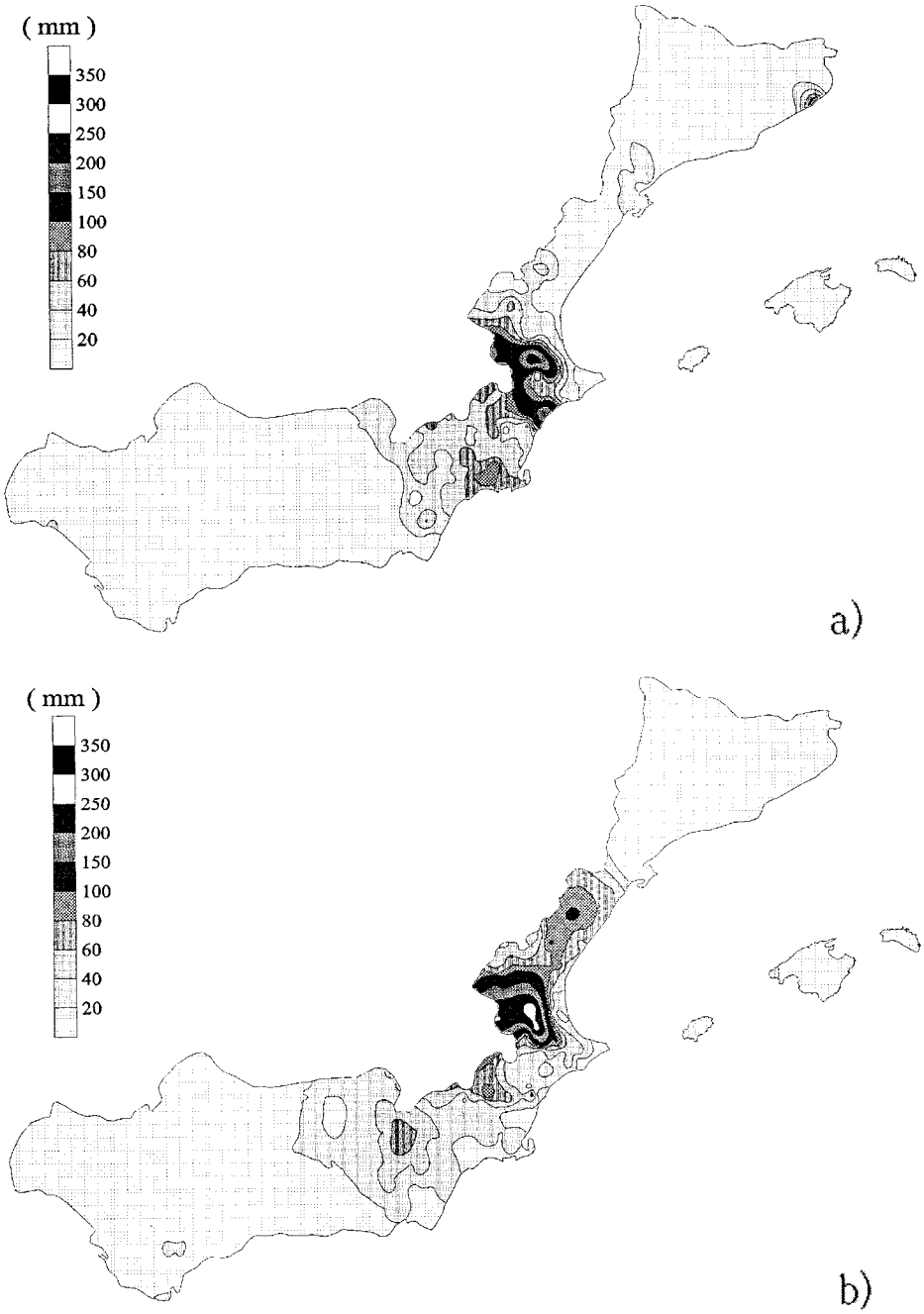

FIG. 9. Analysis of the observed rainfall (mm) in Mediterranean Spain (dark shaded region in Fig. 1) (a) from 0700 UTC 19 Oct to 0700 UTC 20 Oct 1982 and (b) from 0700 UTC 20 Oct to 0700 UTC 21 Oct 1982.

moved northward. Total rainfall for this event exceeded 400 mm at points in central Valencia. Unfortunately, a dam located in the Tous locality (Valencia) broke and caused catastrophic flash floods during the morning of 20 October. Hereinafter, we will refer to this case as the Tous case.

For this event, the synoptic situation at 500 hPa was characterized by a cutoff cyclone with a cold core, centered about Gibraltar Strait and encompassing Morocco, northern Algeria, and most of the Iberian Peninsula (see Fig. 10a, for 0000 UTC 20 October). The higher-latitude flow was much more zonal than for the Gandía case; yet, a positively tilted weak ridge was present over Atlantic Europe. The cutoff low moved approximately 600 km to the southeast during 20 October without experiencing any apparent weakening. Meanwhile, the Eu-

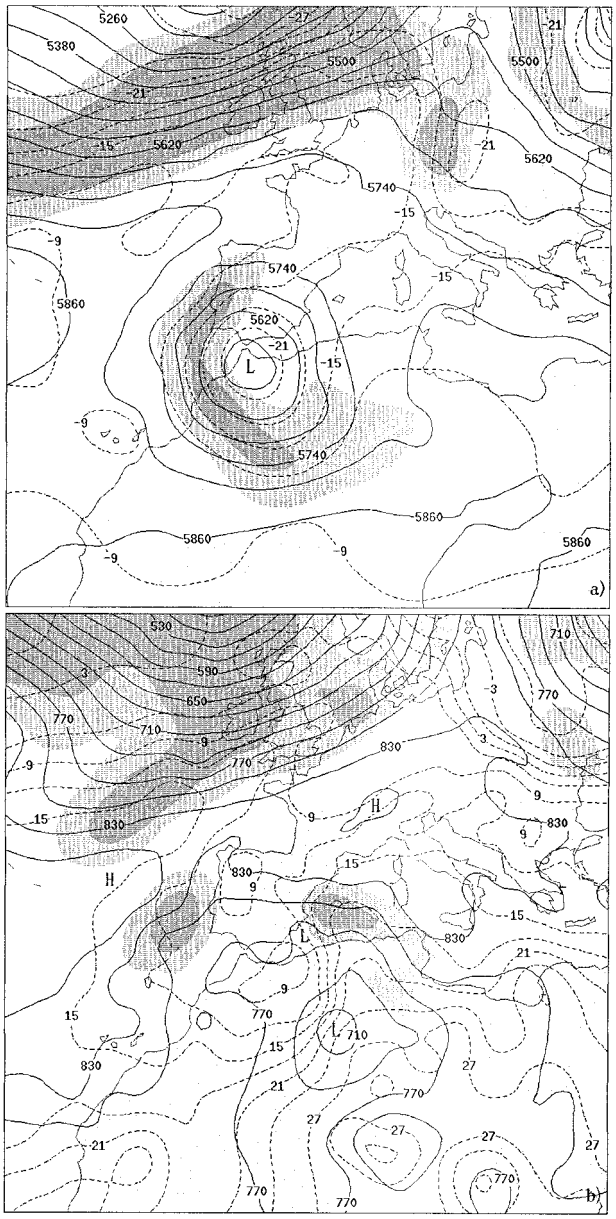

FIG. 10. As in Fig. 5 except for 0000 UTC 20 Oct 1982.

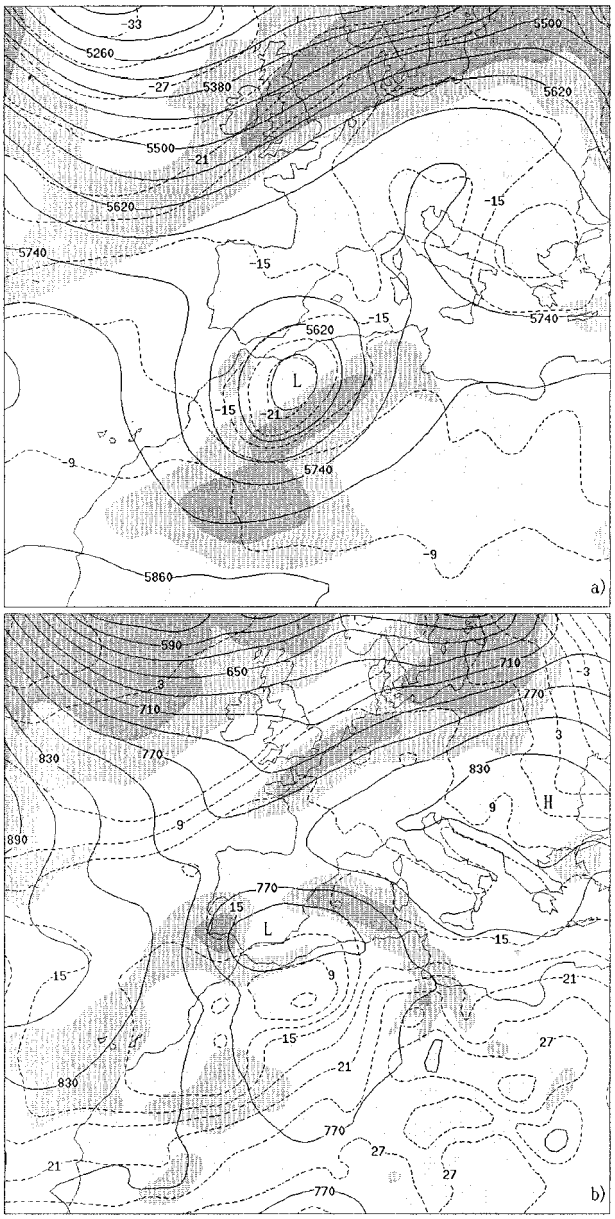

FIG. 11. As in Fig. 5 except for 0000 UTC 21 Oct 1982.

ropean ridge intensified and moved into central Europe (Fig. 11a). The vertical axis of the depression did not exhibit any significant tilting between 750 hPa and the upper troposphere. A jet streak elongated between Portugal and interior Algeria was present around the upper-tropospheric depression at 0000 UTC 20 October (Fig. 10a). During the subsequent hours, the ULJS lifted around the base of the low while a secondary wind maximum, separate from the leading edge of the main ULJS, entered southern Spain and moved from east to west (Fig. 11a).

The evolution at middle- and upper-tropospheric levels was reflected in relatively strong centers of quasi-geostrophic forcing for upward motion (Fig. 12) that rotated in a cyclonic sense over northern Algeria, the southern Mediterranean, and the southern Iberian Peninsula. Rapid pressure falls occurred at lower levels in conjunction with this quasigeostrophic forcing for ascent. As a result, the low pressure center, initially located over a strong baroclinic zone in central Algeria (Fig. 10b), extended to the north and west during 20 October, finally elongating to the south of the Baleric Islands and over the southern Iberian Peninsula and African north coast. The weak anticyclone, initially centered over eastern France, grew in size and moved rapidly to the east (Fig. 11b). Within the general easterly regime over the Mediterranean imposed by this configuration, an intense LLJS was present during the whole event between the

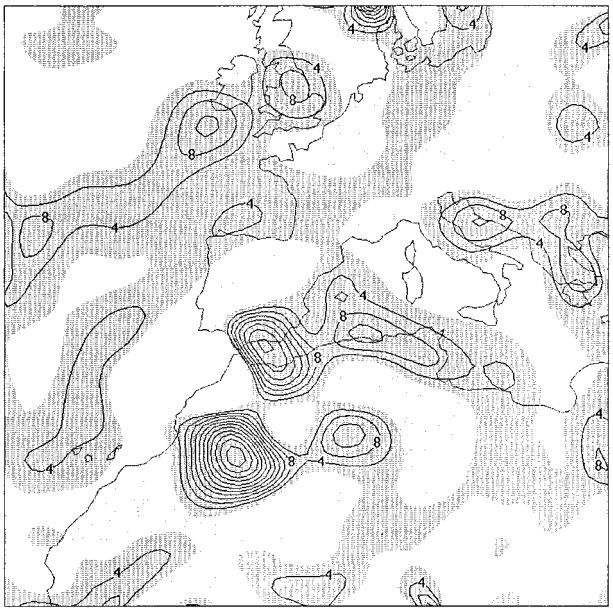

FIG. 12. Areas with upward quasigeostrophic forcing at 500 hPa at 1200 UTC 20 Oct 1982 (shaded). Contour interval is 4×10^{-18} m kg^{-1} s^{-1} starting at 4×10^{-18} m kg^{-1} s^{-1}. The quasigeostrophic forcing is calculated following the *Q*-vector formulation (Hoskins and Pedder 1980).

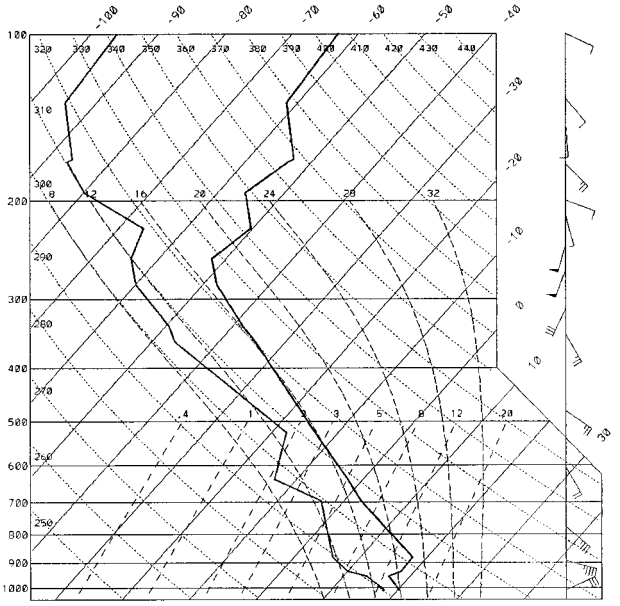

FIG. 13. Radiosounding on 0000 UTC 20 Oct 1982 at Palma (Pa in Fig. 1).

North African coast and Valencia (Fig. 10b). The LLJS wind maximum was constantly over the Balearic Islands. As the surface low moved into southern Spain, the LLJS gained intensity and cyclonic curvature, such that the favorable northeasterly winds over the Sierra de Aitana were established. An interesting feature is that the LLJS coincided approximately with the axis of a thermal ridge present over the western Mediterranean (Fig. 10b), so that warm advection was maximized over that area and eastern Spain. The contrast between the thermal ridge and the cold air tongue present over the Iberian Peninsula and Morocco defined an accentuated front, aligned meridionally between Valencia and interior Algeria at 0000 UTC (Fig. 10b). Within the cyclonic circulation around southeastern Spain, the front rotated cyclonically and by the end of 20 October it was nearly zonally oriented over that area, although appreciably weaker (Fig. 11b). The front was also present at middle and upper levels, approximately aligned with the ULJS of southern Spain mentioned before.

The sounding at Palma (Fig. 13) exhibits the signature of the southeasterly LLJS about 900 hPa, and also a very stable layer capping the surface moist air. In this case, the presence of the stable layer is reflected in a value for the convective inhibition for the surface parcel reaching 192 J kg^{-1}; CAPE is 1243 J kg^{-1}, LI is -1, K is 30, TT is 52, and PW is 32 mm.

The Tous case was characterized by relatively strong dynamical influences from middle- and upper-tropospheric levels. The atypical westward progression of the low pressure center induced at surface, as well as the action of the LLJS and possible frontal forcing, provided continuous low-level convergence over southeastern Spain and Valencia, where abundant moisture supplied by the easterly flow was also available. The possible influence of the Atlas Mountains on the cyclogenesis that took place to the north of these mountains will be investigated in the following sections.

3. Model description and experiments

Further understanding of the Gandía and Tous flash flood events demads an identification and evaluation of mesoscale processes operating within the synoptic context presented in the previous section. For this purpose, several simulations of each event were designed using a nonhydrostatic version of the Pennsylvania State University–National Center for Atmospheric Research Mesoscale Model (Anthes and Warner 1978; Grell et al. 1994).

The model is formulated using the terrain-following σ-coordinate system, with enhanced vertical resolution in the lower troposphere to represent adequately the boundary layer processes. A useful feature of the model is its multiple-nest capability, with two-way interaction between successive nesting levels that allows realistic terrain features (Zhang et al. 1986). For the present simulations, two interacting domains were used, both with $82 \times 82 \times 31$ grid points. The fine grid domain and its orography are those shown in Fig. 1. The domain is centered in the Valencia region and measures 1620 km $\times$ 1620 km under a Lambert conformal map projection (horizontal grid spacing is 20 km). The coarse domain (Fig. 5) measures 4860 km $\times$ 4860 km (grid length 60 km) and is centered at the same location. Time steps

for the fine and coarse grids are 50 and 150 s, respectively. Initial and boundary conditions for the coarse grid are constructed from a first guess produced by horizontal interpolation of the global analysis from NCEP, which is then modified using surface and upper-air observations with a successive-correction objective analysis technique (Benjamin and Seaman 1985). The resulting fields are interpolated to the model σ levels, and initial imbalances of the interpolated fields are reduced by removing the vertical integral of the horizontal divergence in each grid point (Washington and Baumhefner 1975). The initialization process is completed with interpolation of the coarse grid fields to the fine grid.

Simulation of the Gandía case extends 36 h, starting at 0000 UTC 3 November 1987. For the Tous case, the simulation covers 24 h, starting at 0000 UTC 20 October 1982. NCEP global analyses are available at 0000 and 1200 UTC. The tendencies along the model coarse domain boundaries, specified by differences of the fields between those times, are applied using a Newtonian relaxation approach (Grell et al. 1994).

The model incorporates many options for the physical parameterizations. In the present study, the parameterization scheme used to represent the planetary boundary layer physics is a modified version of the Blackadar (1979) scheme (Zhang and Anthes 1982; Zhang and Fritsch 1986). Surface temperature over land is calculated using a force–restore slab model (Blackadar 1979; Zhang and Anthes 1982), and over sea is kept constant during the simulation. Surface fluxes, as well as atmospheric temperature tendencies caused by longwave and shortwave radiation components, are calculated taking into account the cloud cover (Benjamin 1983). Explicit microphysics is represented with predictive equations for cloud water and rainwater below the freezing level, and cloud ice and snow above the freezing level. The scheme includes the effects of hydrostatic water loading, condensation, evaporation, melting, freezing, deposition, and sublimation (Zhang 1989), but not supercooled liquid water. The Betts–Miller parameterization scheme (Betts 1986; Betts and Miller 1986) is chosen to calculate moist convection effects on the coarse grid domain, whereas parameterized convection for the fine grid domain uses the Kain–Fritsch scheme (Kain and Fritsch 1990).

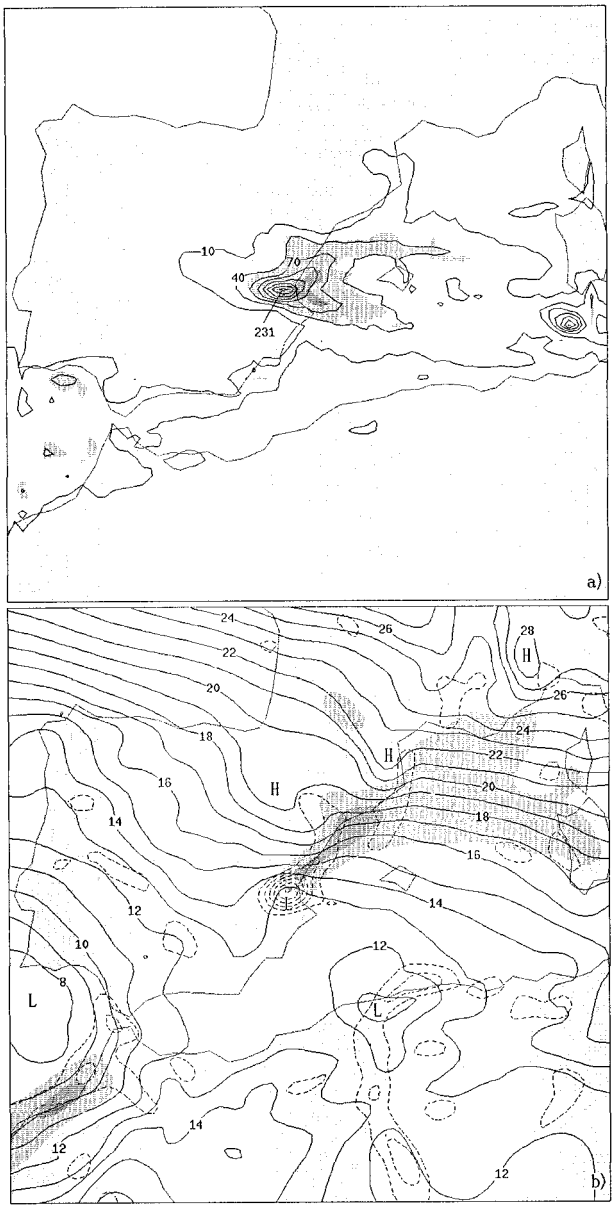

FIG. 14. (a) Forecast total precipitation from 0000 UTC 3 Nov to 1200 UTC 4 Nov 1987. Contour interval is 30 mm, starting at 10 mm (maximum is 231 mm). Areas with continuous precipitation lasting more than 18 and 27 h are shown in light and dark shading, respectively. (b) Model-predicted sea level pressure (continuous line, in hPa without the leading 10 or 100), horizontal wind convergence at 925 hPa (dashed line, contour interval is 5×10^{-5} s^{-1}, starting at 5×10^{-5} s^{-1}), and horizontal wind speed at 925 hPa greater than 15 and 20 m s^{-1} (light and dark shaded, respectively), for 1800 UTC 3 Nov 1987. Lows and highs mentioned in the text are indicated.

4. Mesoscale ingredients

a. Gandía case

Forecast precipitation for this event is shown in Fig. 14a. The model is able to forecast quite accurately the location of the heavy precipitation center in the Valencia region (Fig. 3), but underestimates the peak amount (a forecast maximum of 231 mm versus observations in excess of 600 mm). Further, none of the additional precipitation centers observed farther south are forecast properly, perhaps due to the disorganized convection responsible. The model provides good guidance about the stationarity (measured as the amount of time with uninterrupted rainfall for each grid point) of the convective system that developed over Valencia (nearly 30 h; Fig. 14a).

The ability of the model to capture the location, long

life, and stationarity of the precipitation system seems to be associated with the correct prediction of the large-scale aspects of the circulation and its slow movement. However, the spatial localization and high precipitation efficiency of the system have to be related to the mesoscale ingredients. Indeed, the circulation pattern at low levels is rich in mesoscale components that can plausibly explain the continuous convective development over central Valencia (Fig. 14b). First of all, the low pressure area extending leeward of the Atlas over the Mediterranean, with its center in the Algerian coast, is contributing with an increase of the easterly flow over Valencia as it increases the pressure gradient beyond that which would result solely from the Gulf of Cádiz low. The simulation shows that this secondary low is maintained over the same area, probably owing to the constant interaction of the upper-level flow with the Atlas orography. Embedded within the general low pressure area of the south Mediterranean, there is a mesolow over Valencia, approximately where the heaviest precipitation occurred. Animated sequences of the flow pattern show that the genesis of the mesolow is contemporaneous with the onset of the precipitation over the Gulf of Valencia. Subsequently, it moves downstream approximately in phase with the maximum precipitation, as new troughs develop over the coast in response to new precipitation. This succession of events suggests that the mesolow could be the result of intense latent heat release in the atmospheric column over Valencia. This hypothesis is further supported by the observation of a warm core over that area (temperature field not shown), especially at midtropospheric levels, in agreement with standard radiosonde measurements (Fernández et al. 1995). On the other hand, it is not possible to verify any cyclonic circulation associated with the mesolow with the available density of wind measurements in the area. The mesolow, stimulated by vigorous condensation over central Valencia, is associated with strong low-level convergence and therefore helps to maintain, or enhance, condensation and precipitation, a positive feedback loop. It seems from Fig. 14b that the mesolow is helping to intensify and concentrate the LLJS in its leading part. Once convection is initiated, the LLJS focuses the flow into the sloping terrain of the Sierra de Aitana and produces intense low-level convergence over central Valencia (Fig. 14b) that persists during all the episode.

Other clear features in Fig. 14b are the blocking high pressures found on the windward side of the Alps, Pyrenees, and Iberic system. It is reasonable to argue whether or not the blocking highs induced by the Pyrenees and Iberic system could have favored the event by providing additional channeling of the northeasterly flow toward central Valencia. To investigate this, we performed one simulation with zero orography in the northern half of the Iberian Peninsula to eliminate the action of both mountain systems. The results reveal only slight effects on the rainfall field in central Valencia, in contrast with flash flood situations occurring farther north (e.g., in northern Valencia and coastal Catalonia), where the action of the Pyrenees can be very important (Ramis et al. 1994, 1998).

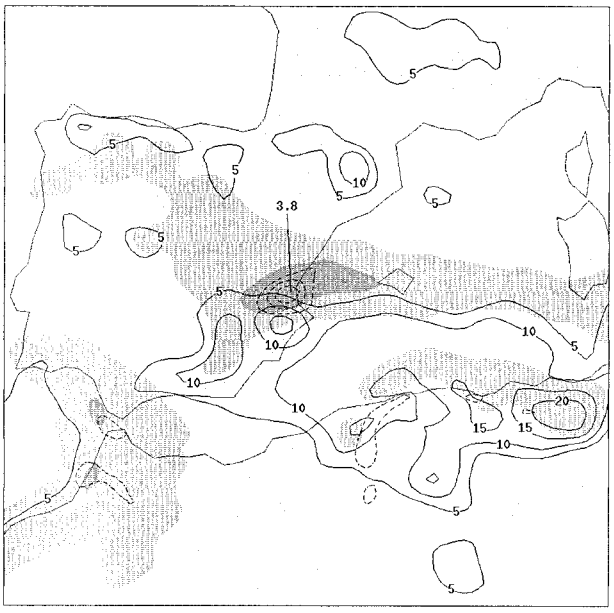

FIG. 15. Convective instability (as measured by the equivalent potential temperature difference between 1000 and 500 hPa, at intervals of 5°C starting at 5°C; continuous line), water vapor flux convergence in the 1000–850-hPa layer (dashed line, contour interval is 1 g m^{-2} s^{-1}, starting at 1 g m^{-2} s^{-1}), and precipitable water greater than 32 and 36 mm (light and dark shaded, respectively), for 1800 UTC 3 Nov 1987.

High values of moisture flux convergence in the lower troposphere are seen over Valencia (Fig. 15). This field is very useful in the diagnosis of flash flood situations since it parameterizes two important ingredients for deep, moist convection: upward motion in the presence of low-level moisture (Barnes and Newton 1986). Calculation of potential or convective instability between 1000 and 500 hPa (solid contours in the same figure) reveals the presence of strong instability over southeastern Spain, the southern Mediterranean, and North Africa. The western part of this region of unstable stratification combines high values of low-level moisture with moderate lapse rates, whereas the eastern part is characterized by drier air, advected from the African plateau, but steep lapse rates. Note that the model-predicted precipitation band over Valencia and the western Mediterranean (Fig. 14a) does not occur in the area of most unstable air, but rather along the boundary between this air and the more stable air to the north. However, the precipitation band nearly coincides with the axis of an east–west-elongated moist tongue present both at low and middle levels. At low levels, the moist tongue is already present at the model initial conditions and is sustained by evaporation from the sea. In midlevels, the tongue developed as very moist air initially present in

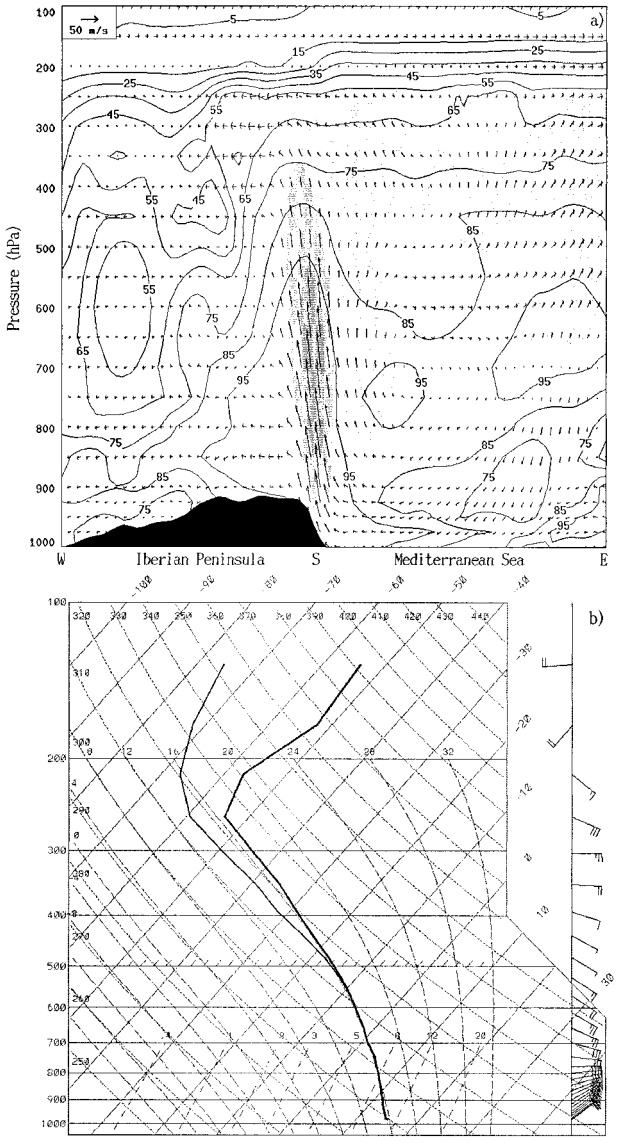

FIG. 16. (a) East–west vertical cross section across the position of maximum horizontal wind convergence at 925 hPa in Fig. 14b. It shows the vector wind field (*u* and *w* components; reference horizontal vector is shown in the upper-left corner), the relative humidity field (in %), and areas with vertical velociy exceeding 5, 25, and 50 cm s^{-1} (light, medium, and dark shaded, respectively), for 1800 UTC 3 Nov 1987. (b) Vertical sounding on a skew *T*–log*p* diagram at point S indicated in (a), for the same time.

the forward flank of the closed low (i.e., over southeastern Spain, the southern Mediterranean, and northern Africa) was advected northward and stretched along the dilatation axis that extends between southern Sardinia and interior Spain (refer to Fig. 5a for an idea of the circulation). The vertical overlap of these moisture distributions defines a band between southern Sardinia and central Spain exhibiting high values of precipitable water, with the maximum always located over Valencia (Fig. 15).

A natural question about this event is to what extent is the local orography responsible for the magnitude of the precipitation over Valencia. Previous case studies of the western Mediterranean region (e.g., Romero et al. 1998) have shown that local orography can be crucial, explaining roughly 90% of the simulated rainfall amounts. It seems evident that upslope flows provided by the mountains of Valencia under the impingement of the easterly/northeasterly winds played a major role also in this case. A vigorous plume of upward motion extending between the surface and 300 hPa is attached to the slopes of the Iberian plateau (Fig. 16a). A time sequence shows that this plume remains approximately rooted to the orography of Valencia with time. Note also the deep layer of high relative humidity that extends above the coastal regions. This feature reflects the deep atmospheric response to the mechanical forcing exerted from beneath, since effective static stability is reduced in moist environments by upslope condensation (Durran and Klemp 1983). Moreover, the presence of a deep plume of very moist air can explain the high precipitation efficiency of this case and also supports the idea that the mesolow of Valencia could be linked to air–condensates latent heat exchange, since evaporative cooling would be highly reduced under these circumstances. It is important to note that the coastal plume of moist, ascending air is also obtained, generally stronger, in a simulation where the convection parameterization scheme is switched off. The results indicate that deep latent heat release associated with resolved-scale condensation promoted over the slopes of Valencia leads to the generation of resolved-scale thermal buoyancy and deep upward motion. In the full simulation, the convective overturning appears to be partitioned between parameterized and explicitly resolved processes, as has been already documented in previous simulations of MCSs (Kain and Fritsch 1998). As in Kain and Fritsch (1998), model vertical soundings in the area where the MCS is simulated indicate the development of layers with moist-absolute instability. In response, grid-scale convection, reflected in mesoscale areas of deep ascent (Fig. 16a) develops, acting to restore the environment toward moist-adiabatic vertical structures (Fig. 16b). A similar plume of deep upward motion was seen in Romero et al. (1998) for their Algeria case.

To obtain a more quantitative description of the importance of the local topography for the event, we performed a new simulation in which the orography of the Iberian Peninsula was removed. The results (not included) show that the rainfall structure of Valencia appears displaced slightly to the north and the peak value is 90 mm (i.e., 40% of that with full orography). This means that dynamical factors as those summarized in Fig. 14b are still sufficiently powerful as to produce heavy precipitation even in the absence of local orographic triggering or enhancements. However, the orographic contribution is substantial.

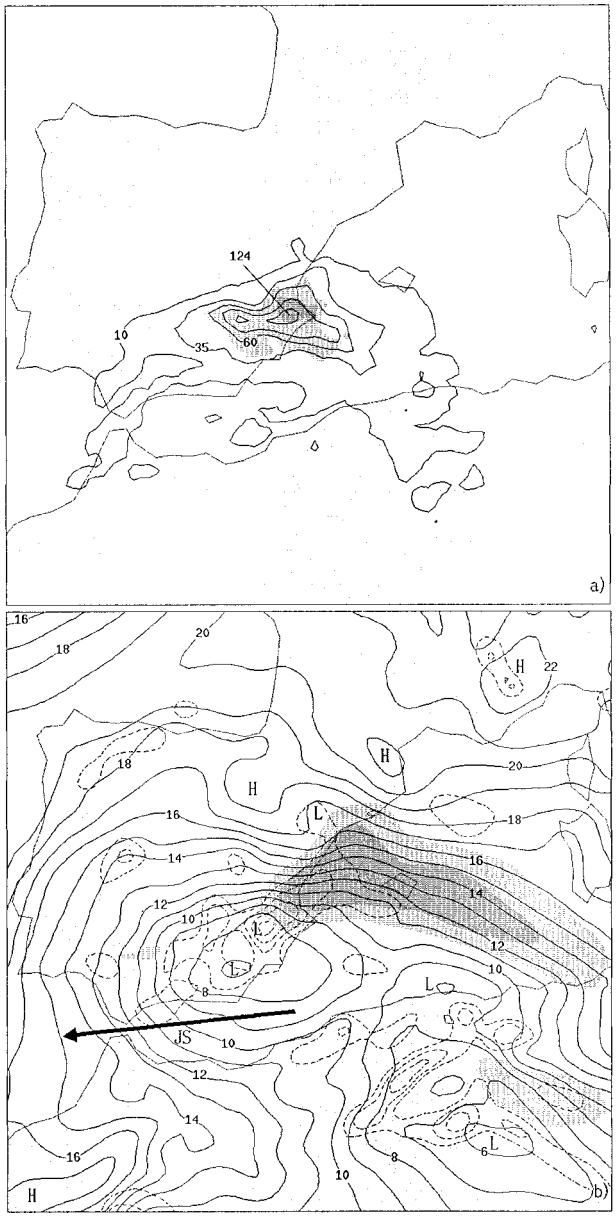

FIG. 17. (a) Forecast total precipitation from 0000 UTC 20 Oct to 0000 UTC 21 Oct 1982. Contour interval is 25 mm, starting at 10 mm (maximum is 124 mm). Areas with continuous precipitation lasting more than 12 and 18 h are shown in light and dark shading, respectively. (b) Model-predicted sea level pressure (continuous line, in hPa without the leading 10 or 100), horizontal wind convergence at 925 hPa (dashed line, contour interval is 5×10^{-5} s^{-1}, starting at 5×10^{-5} s^{-1}), and horizontal wind speed at 925 hPa greater than 15 and 20 m s^{-1} (light and dark shaded, respectively), for 1400 UTC 20 Oct 1982. The arrow represents the ULJS at 300 hPa. Lows and highs mentioned in the text are indicated.

b. Tous case

The skill of the mesoscale model to forecast the spatial structure of the rainfall field is notable for this case (Fig. 17a). A broad area of significant rainfall is predicted over southeastern Spain, where the MCC occurred. Again, rainfall magnitudes are underestimates of actual peak observations (cf. Fig. 9), with the maximum in Valencia reaching 123 mm versus an observed maximum of about 400 mm. The simulation indicates an elongated area of heavy precipitation extending from Sierra de Aitana to the west, where another maximum exists. Such an elongated structure and even the secondary maximum are consistent with the observed rainfall distribution over Valencia (see Fig. 9), although rainfall measurements farther west (unavailable) would be needed for a complete verification. The elongated rainfall structure is also consistent with the shape and position of the most active region of the MCC (Fig. 8). As in that Gandía case, the high stationarity of the convective system is captured well by the model, with precipitation lasting longer than 18 h in the Sierra de Aitana area (Fig. 17a).

The low-level circulation (see Fig. 17b for 1400 UTC) is appreciably stronger, more complex, and faster evolving than for the Gandía event. During the simulation, the low pressure center present over southeastern Spain at 1400 UTC follows a cyclonic trajectory, starting over the interior lands of Algeria (Fig. 18a) and progressing over the southern Mediterranean, southeastern Spain, southern Spain, and ending near the Gibraltar Strait (Fig. 18b). This sequence is associated with a similar evolution of the ULJS, in such a way that the surface low lies below the right entrance region of the ULJS (Figs. 17b and 18). Accordingly, the broad area of significant low-level convergence present over southeastern Spain (dashed contours in the same figure) is vertically associated with strong values of upper-level divergence (field not shown). As commented in section 2 during the synoptic description of the event, the ULJS and surface low occur along a strong baroclinic zone established between warm air to the north that is entering from the Mediterranean, and cold air to the south that came from the western part of the Iberian Peninsula. As shown later, this configuration is reflected in the development of a significant pattern of warm advection to the north and cold advection to the south of southeastern Spain.

As noted in Fig. 17b, the low pressure area in southeastern Spain extends northward toward the area where the heaviest precipitation occurred. That embedded trough seems to be intensifying the LLJS and providing additional convergence. As in the Gandía case, it appears that this pressure perturbation is a consequence of the latent heat release. On the other hand, the influence of the Atlas Mountains in the area of interest is not clear, but it is evident that lee cyclogenesis is taking place to the east of the main low: a stationary low pressure center appears to the southeast of the Balearics over the Algerian coast, as an extension of the larger low located over the African continent. Significant low-level convergence is correspondingly predicted in northern Algeria, an area where deep convection developed (recall Fig. 8). The blocking high pressures induced by

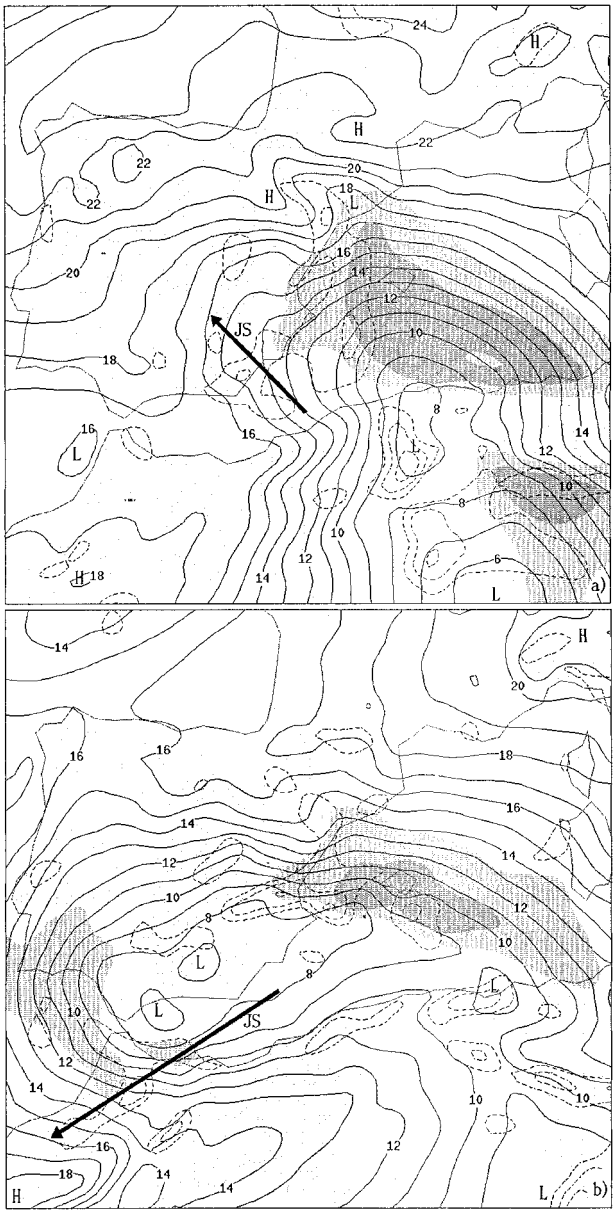

FIG. 18. As in Fig. 17b but for (a) 0400 UTC 20 Oct 1982 and (b) 0000 UTC 21 Oct 1982.

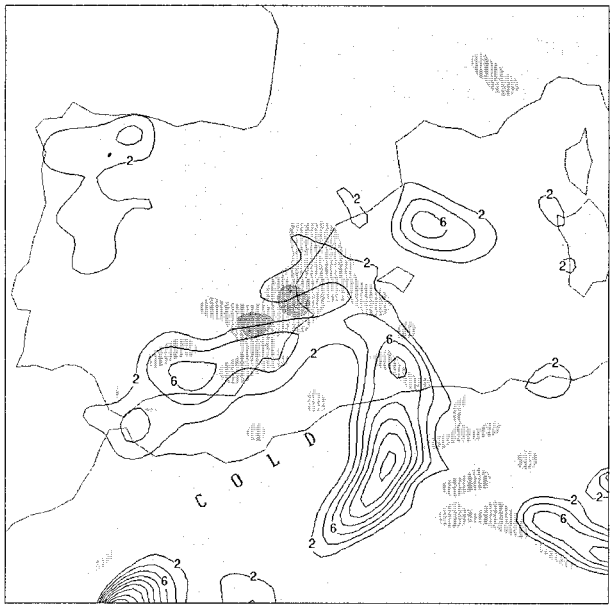

FIG. 19. Integrated frontogenesis and vertical motion in the lower troposphere (1000–700 hPa) for 1400 UTC 20 Oct 1982. Contour interval is 2×10^{-10} K m^{-1} s^{-1}, starting at 2×10^{-10} K m^{-1} s^{-1}. Vertical velocity is shown as light and dark shading for values greater than 5 and 15 cm s^{-1}, respectively.

Atlas, Alps, Pyrenees, and Iberic System are quite pronounced (Fig. 17b), but the simulation without mountains in the northern half of the Iberian Peninsula indicates that the latter two ridges are not relevant for this case either (not shown).

The Pettersen frontogenesis function (Pettersen 1936), or Lagrangian rate of change of the magnitude of the horizontal potential temperature gradient due to the horizontal wind, was calculated from the model output fields. This function, vertically integrated for the lower troposphere, is shown in Fig. 19 for 1400 UTC. Frontogenesis is occurring along an arc-shaped zone connecting southeastern Spain, the Mediterranean, and northern Algeria. In response to the frontogenetic action, a distinct signature of general upward motion is forced toward the warm side (Fig. 19). The frontogenetic activity at low levels and the corresponding upward motion signature were present almost constantly over southeastern Spain, south of the Balearics, and northern Algeria.

Despite the strong evolution of the flow pattern in this case compared to that in Gandía case, ingredients for deep convection remained basically in place for many hours. The zonally elongated shape of the surface depression and its westward progression guaranteed uninterrupted easterly moist flow over eastern Spain, and significant values of low-level moisture flux convergence are indicated by the model in southeastern Spain. In addition, that area is characterized by unstable stratification for moist convection (Fig. 20). These conditions are also met in the other convective areas of northern Algeria. High values of precipitable water (Fig. 20) were generated rapidly over southeastern Spain, owing to the combined action of moist air advection from the Mediterranean at low levels and upward dynamical forcing of this moist air from all tropospheric levels.

An east–west vertical cross section of the circulation (Fig. 21a) reveals the existence of a deep plume of positive vertical velocity above the windward slopes of the mountains of eastern Spain. As with the previous case, this plume is also obtained when the simulation is performed without incorporating the convective scheme, since the plume develops mainly in response to deep latent heat release by the gridscale condensation. Model-

FIG. 20. Convective instability (as measured by the equivalent potential temperature difference between 1000 and 500 hPa, at intervals of 5°C starting at 5°C; continuous line), water vapor flux convergence in the 1000–850-hPa layer (dashed line, contour interval is 1 g m^{-2} s^{-1}, starting at 1 g m^{-2} s^{-1}), and precipitable water greater than 36 and 40 mm (light and dark shaded, respectively), for 1400 UTC 20 Oct 1982.

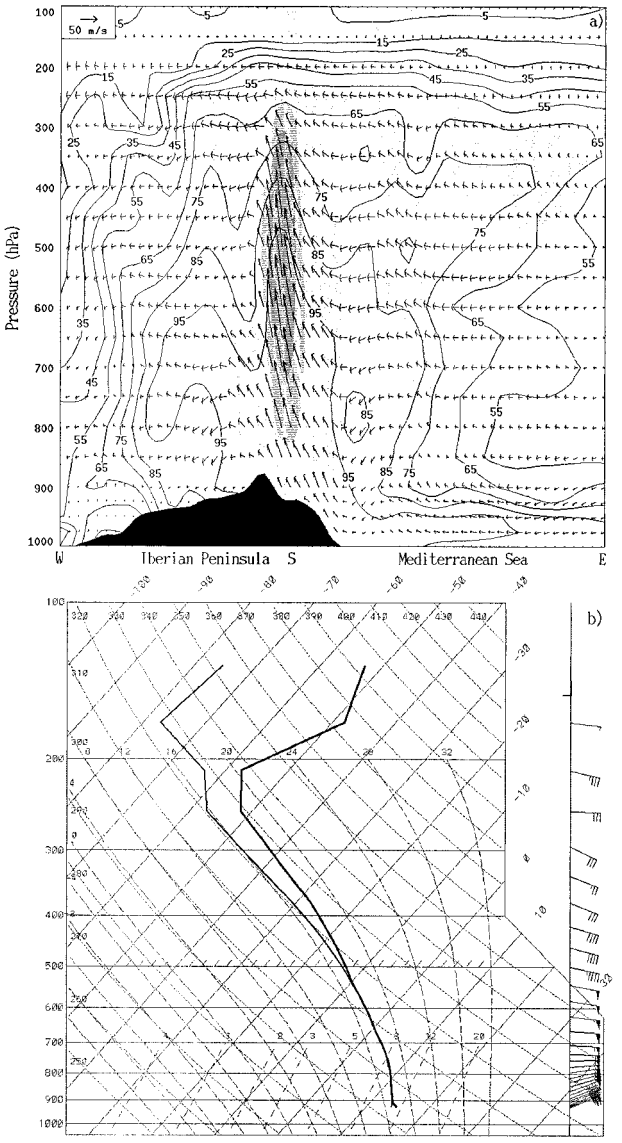

FIG. 21. East–west vertical cross section across the position of maximum horizontal wind convergence at 925 hPa in Fig. 17b. It shows the vector wind field (*u* and *w* components; reference horizontal vector is shown in the upper-left corner), the relative humidity field (in %), and areas with vertical velocity exceeding 5, 35, and 70 cm s^{-1} (light, medium, and dark shaded, respectively), for 1400 UTC 20 Oct 1982. (b) Vertical sounding on a skew *T*–log*p* diagram at point S indicated in (a), for the same time.

predicted vertical soundings in southeastern Spain exhibit moist-absolute instability at some times (Fig. 21b), a clear indication of multiscale (explicit and parameterized) convective overturning (Kain and Fritsch 1998). The upward motion signal is notably stronger and more elevated than for the Gandía event, probably owing to the greater contribution of synoptic-scale dynamical forcings. In effect, the simulation run after eliminating the orography of the Iberian Peninsula indicates that maximum rainfall amounts, nearly located in the same place, are reduced by only 30% in this case. On the other hand, the high values of relative humidity predicted by the model over the area of interest (Fig. 21a) would also imply in this case relatively minor effects of evaporation.

5. Effects of Atlas orography and latent heat exchange

Guided by the results of the previous control experiments, it was suggested in the previous section that the effects of Atlas orography and latent heat exchange could have been relevant for both case studies. It was hypothesized that to some extent, the general pressure depression in the southern Mediterranean and the apparent embedded troughing in the Valencia area were due to these factors. It seems logical that these structures helped to sustain the onshore advection and low-level convergence necessary for an efficient feeding of the convective systems developed over central Valencia. To investigate these ideas in a more rigorous and quantitative way, we devote this section to a factor separation study by means of numerical simulations.

Consider first one simulation where both factors are eliminated. That is, the North African orography is removed prior to the initialization of the model, and latent heating terms (both absorption and release by the water phases) appearing in the temperature tendency equation are explicitly set to zero.

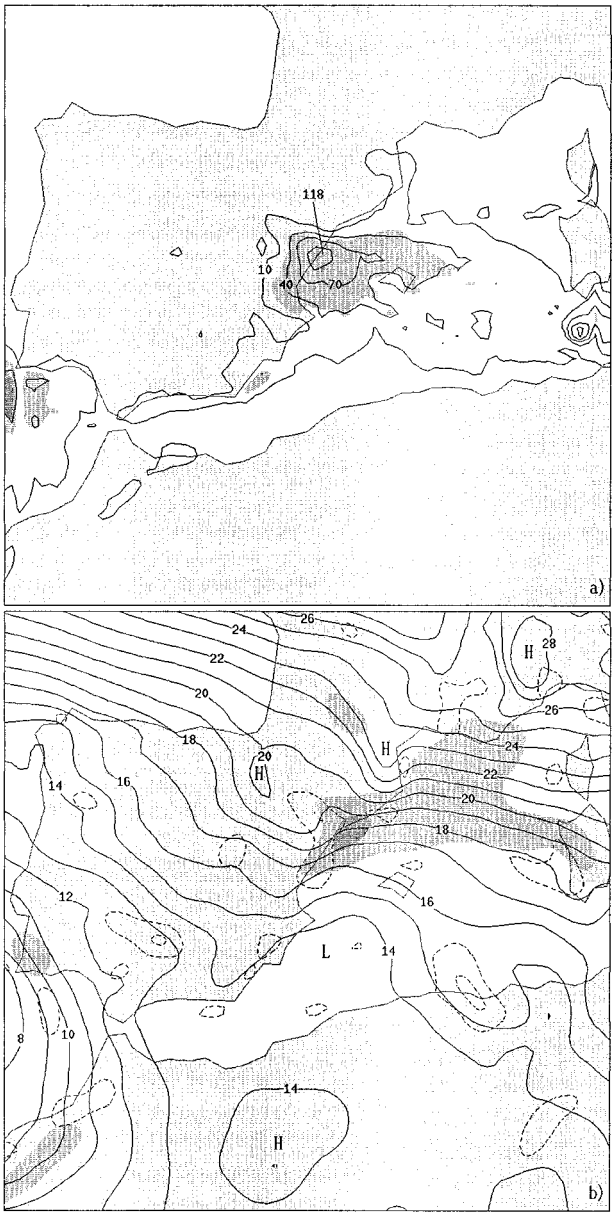

FIG. 22. (a) As in Fig. 14a and (b) as in Fig. 14b but for the simulation excluding both Atlas orography and latent heat exchange.

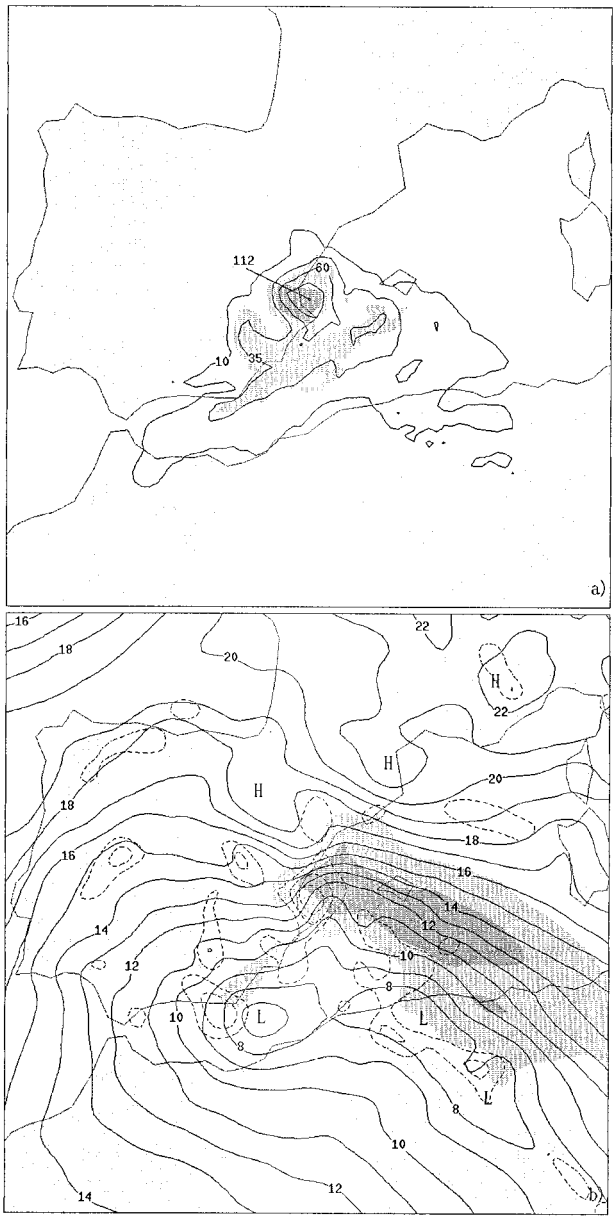

FIG. 23. (a) As in Fig. 17a and (b) as in Fig. 17b but for the simulation excluding both Atlas orography and latent heat exchange.

For the Gandía event (Fig. 22), the results differ appreciably from the control experiment (Fig. 14). First of all, the resulting precipitation field is displaced toward the coast of northern Valencia, with a general suppression of rainfall in central Valencia and the complete disappearance of the inland peak. Accordingly, the low-level circulation (Fig. 22b) is characterized by the LLJS and downstream convergence concentrated toward northern Valencia, and much less intense maritime flow and convergence in central Valencia. Note that although the sea level pressure over the southern Mediterranean and southern Spain is higher than in the full experiment (Fig. 14b), a relative low pressure area still appears over the southern Mediterranean. Without rejecting any other possible dynamical reason for that low pressure area, it is obvious that Atlas effects do not disappear entirely by removing their orography during the simulation; the initial fields are based on analyses and actual observations that, in turn, contain orographic effects. Surface vorticity centers present at initial time, although no longer sustained by the ridge, are still influencing the forecast to some degree.

For the Tous event (Fig. 23), large differences are also observed, when both the Atlas Mountains orography and latent heat effects are removed, in comparison with the full experiment (Fig. 17). The rainfall maxi-

TABLE 1. Summary of the numerical experiments performed for each case study in order to isolate the effects of the Atlas Mountains and latent heat exchange.

Experiment	Atlas orography	Latent heat exchange
f_0	No	No
f_1	Yes	No
f_2	No	Yes
f_{12}	Yes	Yes

mum is moved slightly to the northeast, toward the waters of Gulf of Valencia and inland precipitation is much reduced, with the omission of the elongated structure and western maximum observed in Fig. 17a. Also, the position of the LLJS shifts southward, and its leading extremum is now focused toward the Gulf of Valencia, where a strong convergence signal exists. Notably, the low pressure area centered over southeastern Spain in the full experiment (Fig. 17b) is now centered over the southern Mediterranean, and low-level convergence over the lands of southeastern Spain is much weaker. The general sea level pressure increase noted northward of the Atlas in the Gandía simulation is not observed in this case.

Therefore, the previous simulations point out the notable effect that these factors have on the evolution of both events. This result is obtained through (a) the action of the Atlas orography irrespectively of latent-heat-induced processes, or (b) by the action of latent heat exchanges irrespectively of the presence of the Atlas Mountains, or (c) by the interaction between the two factors. The partitioning of the total effect among these independent contributions can be assessed following the method of Stein and Alpert (1993). The output (e.g., rainfall) of the full experiment (f_{12}), the experiment excluding both Atlas orography and latent heat exchange (f_0), and the two additional experiments f_1 and f_2 (see Table 1 for a description) can be combined algebraically to yield the desired contributions:

- effect of the Atlas orography, $f_1^* = f_1 - f_0$;
- effect of the latent heat exchange, $f_2^* = f_2 - f_0$; and
- effect of the interaction, Atlas and latent heat, $f_{12}^* = f_{12} - (f_1 + f_2) + f_0$.

Below, we present these contributions for each case study.

a. Gandía case

The effects of Atlas orography on the sea level pressure and low-level wind field for a representative time (2100 UTC), and on the total precipitation, are shown in Fig. 24a. The Atlas Mountains induce an extensive pressure decrease over the Mediterranean, with the maximum action about the Algerian coast. This pressure pattern modifies the circulation in the sense of favoring cyclogenesis in the southern Mediterranean and intensifying the easterly flow from southern Sardinia to central Valencia. Convergence zones tend to be shifted to the south and this is reflected in a band of rainfall suppression to the north of the Balearics in favor of rainfall enhancement to the south. In particular, the Atlas Mountains act to reduce rainfall production in northern Valencia and to increase it in the central part of the region. The Atlas Mountains also influence the circulation in the Morocco area; cyclogenesis is induced around the Gulf of Cádiz (leading to rainfall enhancement in the Gibraltar Strait area), whereas positive pressure anomalies are induced over Morocco.

The effect of latent heat (Fig. 24b) on the pressure pattern is significantly negative for most of the eastern part of the Iberian Peninsula. The maximum negative contribution occurs over Valencia and this induces the development of an intense mesoscale cyclonic circulation and strong convergence. A time series shows that these structures tend to move downstream toward inland Spain, but new ones are readily generated over the Valencia area. As a result, the effect on the precipitation field is very important and basically positive over the area of interest. The latent heat factor is focusing the rainfall over Valencia, slightly to the north of the forecast maximum (Fig. 14a).

The interaction of the Atlas orography and latent heat factors defines a more complex pattern, both in space and time, of the analyzed fields (Fig. 24c). This is typical, given the synergistic nature of the causal processes. Unfortunately, the virtue of the factor separation technique that permits the isolation of synergistic effects does not guarantee an easy interpretation of these interaction terms. Nevertheless, the interaction effect on the rainfall field over Valencia seems to follow a similar tendency to the Atlas Mountains effect, that is, a southward shift of the rainfall activity. This implies a strengthening and displacement to the south (nearly at the location of the forecast maximum) of the rainfall induced by the latent heat factor. The interaction effect on the pressure pattern and circulation is much weaker and variable, although negative pressure contributions are present most of the time over southern Spain.

b. Tous case

The effect of Atlas Mountains (Fig. 25a) on the sea level pressure field does not follow the same pattern found for the Gandía case. Negative contributions are present over the Mediterranean about and to the east of the Balearics, but not in the remaining areas. To the west, over southern Spain, the Mediterranean, and northern Africa, the anomalies induced by the Atlas Mountains are positive. This pattern implies that the easterly flow over the Mediterranean is not so extensively favored. Enhancement of the easterlies is constrained to the east of the Balearics; over eastern Spain, the Atlas Mountains induce northerly winds and offshore outflows, both of which are certainly unfavorable for rainfall enhancement. Under these circumstances,

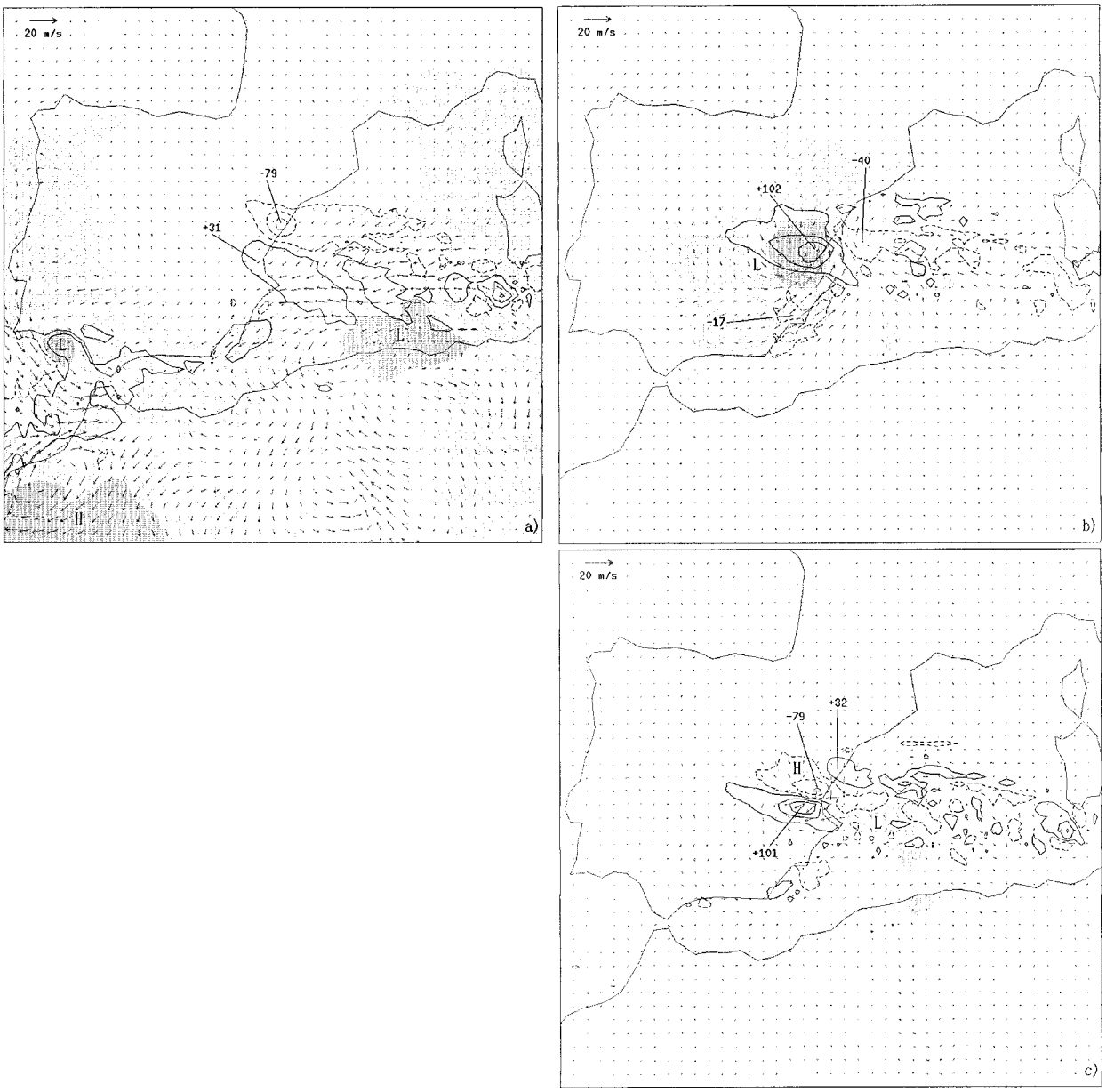

FIG. 24. Factor separation results for the Gandía case. Effects of (a) Atlas orography, (b) latent heat exchange, and (c) interaction of Atlas orography–latent heat exchange, on the fields: total precipitation, for which contour interval is 30 mm, starting at 10 mm for positive contributions (continuous line), and at −10 mm for negative contributions (dashed line) (some maxima are also indicated); vector wind field at 925 hPa at 2100 UTC 3 Nov 1987 (reference vector is shown in the upper-left corner); and sea level pressure at 2100 UTC 3 Nov 1987 (light and dark shading represent contributions greater than 0.5 and 2 hPa, respectively, with L indicating zones of negative contribution and H zones of positive contribution).

the effect of the Atlas orography on the total precipitation field turns out to be weak for this case and, interestingly, basically negative in the Mediterranean and Valencia (Fig. 25a). The synergistic effect (Fig. 25c), although more complex in space and time, is finally expressed in a rainfall reduction over most of the areas of eastern Spain.

These results pose an exception to the customary scenario in which the effect of the Atlas Mountains favors heavy rainfall in particular zones of eastern Spain. Note that, unlike the Gandía case, where the upper-level winds have a substantial component normal to the ridge during the entire episode (Fig. 5a), for the Tous case the cutoff low is initially located more to the east and is moving eastward (Figs. 10a and 11a). Therefore, the favorable southerly winds for Mediterranean cyclogenesis occur only toward the eastern part of the ridge. Also, it is possible, though unclear in the procedure,

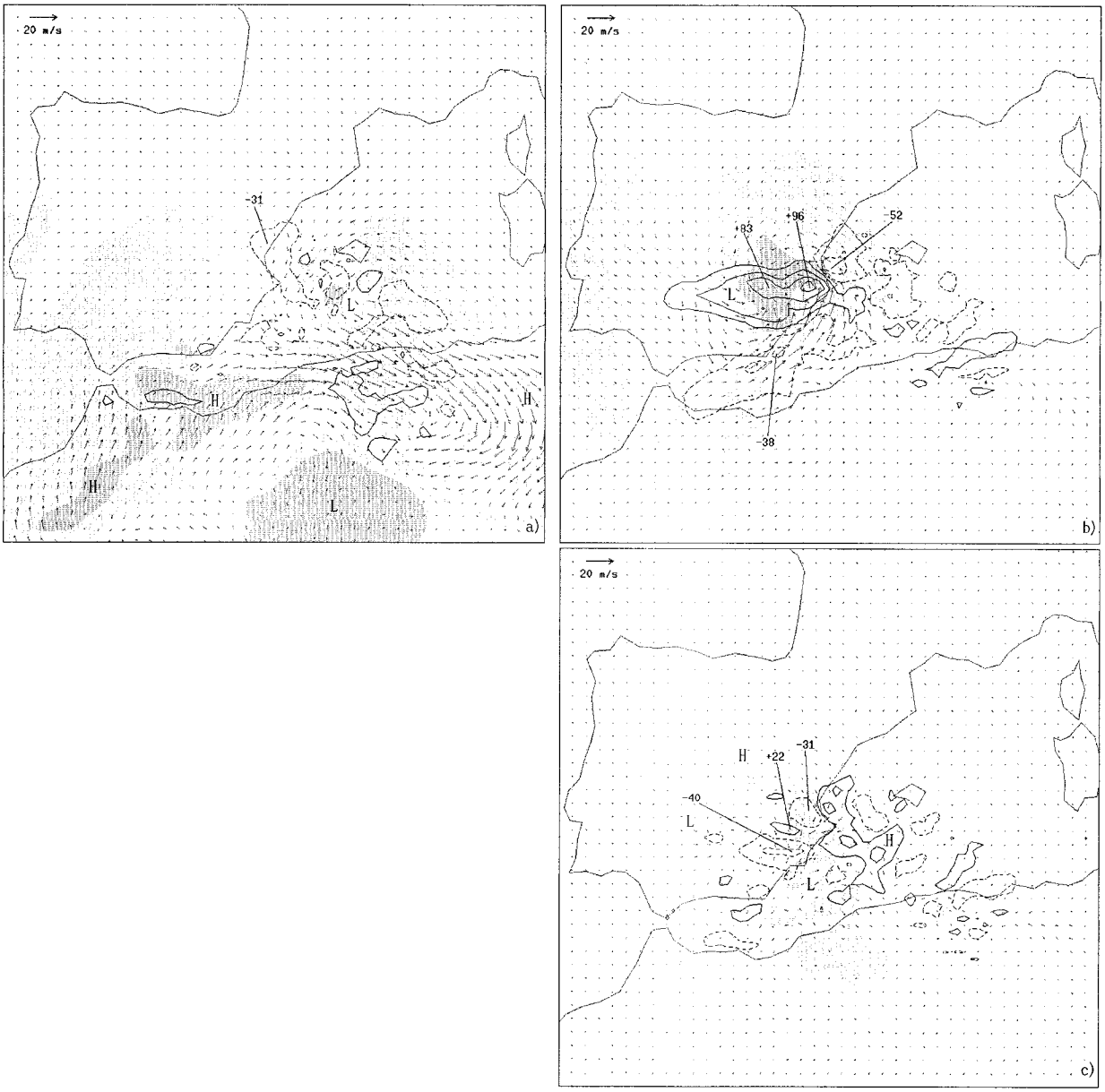

FIG. 25. Factor separation results as in Fig. 24 except for Tous case (contour interval for total precipitation is 25 mm, and representative time for wind and sea level pressure is 1000 UTC 20 Oct 1982).

that the special nature of the surface circulation in this case, driven by strong upper-level dynamics and appreciable baroclinicity of the flow, does not need the modulation provided by the Atlas to operate properly, or even is negatively disrupted by the presence of the ridge.

On the other hand, Fig. 25b shows that the feedback between latent-heat-induced processes and the event itself was extraordinarily positive. The latent heat factor explains a substantial fraction of the interior precipitation. It defines the elongated structure and two maxima observed in the control forecast (Fig. 17a). This positive rainfall signal is developed along a strong convergence line defined by the intense vortex created over southeastern Spain. A time sequence of the fields shows that negative pressure anomalies are continuously excited over Valencia and Murcia, which then propagate downstream affecting the circulation and defining or strengthening convergence zones (Fig. 25b).

6. Conclusions

In this paper, a mesoscale numerical study of two catastrophic flash flood events in eastern Spain has been carried out, putting special emphasis on those aspects of the synoptic and mesoscale settings that could explain the high stationarity and efficiency of the responsible

convective systems. The analysis indicates some synoptic-scale similarities between the events (cold-core closed lows aloft about southern Spain and a long fetch of flow over the Mediterranean interacting with the terrain features of eastern Spain), but at the same time stresses the unique characteristics of each event. One of the events (3–4 November 1987) developed within a long-lasting and dynamically weak synoptic context. The other MCS (20 October 1982) did not occur within such ''static'' conditions, but under relatively strong dynamic forcing at middle and upper levels and appreciable baroclinicity of the flow. In the first case, the stationary character of the convective system seems to be linked to the stagnancy of the large-scale pattern itself; in the second case, the persistent easterly moist flow and upward forcing are due to the peculiar behavior of the disturbance (mobile, but along a cyclonic path about the southern Mediterranean).

The simulations presented, along with previous studies, confirm that mesoscale models can be a valuable forecasting tool for these extreme situations, as they provide generally good guidance about the spatial and temporal distribution of rainfall. To a certain extent, this is expected owing to the amount of predictability facilitated by the complex topography of the western Mediterranean; most of the flash floods in the area are associated with MCSs triggered or sustained by coastal orographic lifting. In the simulations, the coastal orography promotes a deep and intense plume of upward motion through development of moist-absolute instability and gridscale convection in addition to parameterized convection. This results in very important amounts of rain. However, as is typical of the situations dominated by deep convection, rainfall amounts are systematically underforecast. For that reason, any operational implementation of mesoscale models for the forecasting and vigilance of flooding situations in the area should be followed by a parallel research effort aimed at improvement of quantitative precipitation forecasts.

Besides the recognized importance of the local topography, our numerical experiments emphasize the relevant role exerted by other mesoscale factors. For the event of 3–4 November 1987, the modulation of the low-level circulation over the Mediterranean induced by the Atlas ridge was shown to be important. This modulation, caused by the cyclogenetic action leeward of the ridge, determined an enhancement of the easterly flow and horizontal convergence toward central Valencia, supposing a localization of rainfall in that place at the expense of other areas farther north. This result fits the classical conceptual model of flash flood situations in eastern Spain, which includes the shallow north Algerian cyclone as an essential component. However, the confluence of the proper physical ingredients for the genesis of heavy precipitation on a particular place and time can be achieved in a number of different ways by the atmosphere. Conceptual models are useful and can be statistically justified, but are subject to exception. As an example, our second case study indicates that the action of the Atlas Mountains was irrelevant or even negative.

On the other hand, the investigation of the effects of atmospheric diabatic heating due to latent heat release revealed a strongly positive interaction of this factor with both events. A mesoscale cyclonic circulation that developed in the areas of heavy precipitation affected the parent circulation strongly, enhancing the horizontal convergence ahead of the LLJS. These structures were continuously redeveloped in fixed areas of Valencia and Murcia owing to the stationarity of the precipitation system, thus resulting in strong rainfall localization in inland areas. These results reinforce the notion that the forecast of flooding situations requires not only a proper identification of ingredients prior to the development of convection, but also a close tracking and monitoring of the event after the onset of precipitation, trying to identify new elements that could endow the convective system with additional organization, efficiency, or longevity.

Acknowledgments. We gratefully acknowledge constructive comments on an earlier version of this manuscript from Dr. Conrad Ziegler and Mr. Richard Thompson. This work was performed while the first author held a National Research Council–National Severe Storms Laboratory Research Associateship. Also, computer support provided by NCAR/Scientific Computer Division (which is sponsored by the National Science Foundation) for meteorological data preprocessing is acknowledged. Precipitation data and Meteosat satellite pictures for the documentation of the cases were provided by the Spanish Instituto Nacional de Meteorología.

REFERENCES

Anthes, R. A., and T. T. Warner, 1978: Development of hydrodynamic models suitable for air pollution and other mesometeorological studies. *Mon. Wea. Rev.,* **106,** 1045–1078.

Barnes, S. L., and C. W. Newton, 1986: Thunderstorms in the synoptic setting. *Thunderstorm Morphology and Dynamics,* 2d ed., E. Kessler, Ed., University of Oklahoma Press, 75–112.

Benjamin, S. G., 1983: Some effects of heating and topography on the regional severe storm environment. Ph.D. thesis, The Pennsylvania State University, 265 pp. [Available from University Microfilm, 300 N. Zeeb Rd., P.O. Box 1346, Ann Arbor, MI 46801-1346.]

——, and N. L. Seaman, 1985: A simple scheme for improved objective analysis in curved flow. *Mon. Wea. Rev.,* **113,** 1184–1198.

Betts, A. K., 1986: A new convective adjustment scheme. Part I: Observational and theoretical basis. *Quart. J. Roy. Meteor. Soc.,* **112,** 677–692.

——, and M. J. Miller, 1986: A new convective adjustment scheme. Part II: Single column tests using GATE wave, BOMEX, ATEX and Arctic air-mass data sets. *Quart. J. Roy. Meteor. Soc.,* **112,** 693–709.

Blackadar, A. K., 1979: High resolution models of the planetary boundary layer. *Advances in Environmental Science and Engi-*

neering, Vol. 1, No. 1, J. Pfafflin and E. Ziegler, Eds., Gordon and Breach, 50–85.

Chappell, C. F., 1986: Quasi-stationary convective events. *Mesoscale Meteorology and Forecasting,* P. S. Ray, Ed., Amer. Meteor. Soc., 289–310.

Doswell, C. A., III, 1987: The distinction between large-scale and mesoscale contribution to severe convection: A case study example. *Wea. Forecasting,* **2,** 3–16.

——, C. Ramis, R. Romero, and S. Alonso, 1998: A diagnostic study of three heavy precipitation episodes in the western Mediterranean region. *Wea. Forecasting,* **13,** 102–124.

Durran, D. R., and J. B. Klemp, 1983: A compressible model for the simulation of moist mountain waves. *Mon. Wea. Rev.,* **111,** 2341–2361.

Emanuel, K. A., 1983: On assessing local conditional symmetric instability from atmospheric soundings. *Mon. Wea. Rev.,* **111,** 2016–2033.

Farrell, R. J., and T. N. Carlson, 1989: Evidence for the role of the lid and underrunning in an outbreak of tornadic thunderstorms. *Mon. Wea. Rev.,* **117,** 857–871.

Fernández, C., M. A. Gaertner, C. Gallardo, and M. Castro, 1995: Simulation of a long-lived meso-β scale convective system over the mediterranean coast of Spain. Part I: Numerical predictability. *Meteor. Atmos. Phys.,* **56,** 157–179.

Font, I., 1983: *Climatología de España y Portugal.* Instituto Nacional de Meteorología, 296 pp. [Available from Instituto Nacional de Meteorología, Apartado 285, 28071 Madrid, Spain.]

Grell, G. A., J. Dudhia, and D. R. Stauffer, 1994: A description of the fifth-generation Penn State/NCAR mesoscale model (MM5). NCAR Tech. Note NCAR/TN-398+STR, 117 pp.

Hakim, G. J., and L. W. Uccellini, 1992: Diagnosing coupled jet streak circulations for a northern plains snow band from the operational nested-grid model. *Wea. Forecasting,* **7,** 26–48.

Homar, V., C. Ramis, R. Romero, S. Alonso, J. A. García Moya, and M. Alarcón, 1999: A case of convection development over the western Mediterranean Sea: A study through numerical simulations. *Meteor. Atmos. Phys.,* **71,** 169–188.

Hoskins, B. J., and M. A. Pedder, 1980: The diagnosis of middle latitude synoptic development. *Quart. J. Roy. Meteor. Soc.,* **106,** 707–719.

Kain, J. S., and J. M. Fritsch, 1990: A one-dimensional entraining/detraining plume model and its application in convective parameterization. *J. Atmos. Sci.,* **47,** 2784–2802.

——, and ——, 1998: Multiscale convective overturning in mesoscale convective systems: Reconciling observations, simulations, and theory. *Mon. Wea. Rev.,* **126,** 2254–2273.

Maddox, R. A., 1980: Mesoscale convective complexes. *Bull. Amer. Meteor. Soc.,* **61,** 1374–1387.

——, L. R. Hoxit, C. F. Chappell, and F. Caracena, 1978: Comparison of meteorological aspects of the Big Thompson and Rapid City floods. *Mon. Wea. Rev.,* **106,** 375–389.

——, C. F. Chappell, and L. R. Hoxit, 1979: Synoptic and meso-α scale aspects of flash flood events. *Bull. Amer. Meteor. Soc.,* **60,** 115–123.

Pettersen, S., 1936: Contribution to the theory of frontogenesis. *Geofys. Publ.,* **11** (6), 1–27.

Ramis, C., M. C. Llasat, A. Genovés, and A. Jansá, 1994: The October-1987 floods in Catalonia: Synoptic and mesoscale mechanisms. *Meteor. Appl.,* **1,** 337–350.

——, R. Romero, V. Homar, S. Alonso, and M. Alarcón, 1998: Diagnosis and numerical simulation of a torrential precipitation event in Catalonia (Spain). *Meteor. Atmos. Phys.,* **69,** 1–21.

Riosalido, R., 1990: Characterization of mesoscale convective systems by satellite pictures during PREVIMET MEDITERRANEO-89 (in Spanish). *Proc. Segundo Simposio Nacional de Predicción,* Madrid, Spain, Instituto Nacional de Meteorología, 135–148. [Available from Instituto Nacional de Meteorología, Apartado 285, 28071 Madrid, Spain.]

——, A. Rivera, and F. Martín, 1988: Development of a mesoscale convective system in the Spanish mediterranean area. *Proc. Seventh Meteosat Scientific Users' Meeting,* Madrid, Spain, EUMETSAT, 375–378.

Rivera, A., and R. Riosalido, 1986: Mediterranean convective systems as viewed by Meteosat. A case study. *Proc. Sixth Meteosat Scientific Users' Meeting,* Amsterdam, Netherlands, EUMETSAT, 101–104.

Rockwood, A. A., and R. A. Maddox, 1988: Mesoscale and synoptic interactions leading to intense convection: The case of 7 June 1982. *Wea. Forecasting,* **3,** 51–68.

Romero, R., 1998: Numerical simulation of mesoscale processes in the western Mediterranean: Environmental impact and natural hazards. Ph.D. thesis, Universitat de les Illes Balears, 164 pp. [Available from University Microfilm, Biblioteca Edif. Mateu Orfila, Universitat de les Illes Balears, 07071 Palma de Mallorca, Spain.]

——, C. Ramis, and S. Alonso, 1997: Numerical simulation of an extreme rainfall event in Catalonia: Role of orography and evaporation from the sea. *Quart. J. Roy. Meteor. Soc.,* **123,** 537–559.

——, ——, ——, C. A. Doswell III, and D. J. Stensrud, 1998: Mesoscale model simulations of three heavy precipitation events in the western Mediterranean region. *Mon. Wea. Rev.,* **126,** 1859–1881.

——, G. N. Sumner, C. Ramis, and A. Genovés, 1999: A classification of the atmospheric circulation patterns producing significant daily rainfalls in the Spanish Mediterranean area. *Int. J. Climatol.,* **19,** 765–785.

Smith, R. B., 1989: Hydrostatic airflow over mountains. *Advances in Geophysics,* Vol. 31, Academic Press, 1–41.

Stein, U., and P. Alpert, 1993: Factor separation in numerical simulations. *J. Atmos. Sci.,* **50,** 2107–2115.

Stensrud, D. J., and J. M. Fritsch, 1993: Mesoscale convective systems in weakly forced large-scale environments. Part I: Observations. *Mon. Wea. Rev.,* **121,** 3326–3344.

Uccellini, L. W., 1975: A case study of apparent gravity waves initiation of severe convection storms. *Mon. Wea. Rev.,* **103,** 497–513.

——, and D. R. Johnson, 1979: The coupling of upper and lower jet streaks and implications for the development of severe convective storms. *Mon. Wea. Rev.,* **107,** 682–703.

Washington, W. M., and D. P. Baumhefner, 1975: A method of removing Lamb waves from initial data for primitive equation models. *J. Appl. Meteor.,* **14,** 114–119.

Weaver, J. F., 1979: Storm motion as related to boundary-layer convergence. *Mon. Wea. Rev.,* **107,** 612–619.

Zhang, D. L., 1989: The effect of parameterized ice microphysics on the simulation of vortex circulation with a mesoscale hydrostatic model. *Tellus,* **41A,** 132–147.

——, and R. A. Anthes, 1982: A high-resolution model of the planetary boundary layer. Sensitivity tests and comparisons with SESAME-79 data. *J. Appl. Meteor.,* **21,** 1594–1609.

——, and J. M. Fritsch, 1986: Numerical simulation of the meso-β scale structure and evolution of the 1977 Johnstown flood. Part I: Model description and verification. *J. Atmos. Sci.,* **43,** 1913–1943.

——, H. R. Chang, N. L. Seaman, T. T. Warner, and J. M. Fritsch, 1986: A two-way interactive nesting procedure with variable terrain resolution. *Mon. Wea. Rev.,* **114,** 1330–1339.